

Burning Characteristics of Individual Douglas-Fir Trees in the Wildland/Urban Interface

by

Elisa Schulz Baker

A Thesis

Submitted to the Faculty

of the

WORCESTER POLYTECHNIC INSTITUTE

In partial fulfillment of the requirements for the

Degree of Master of Science

in

Fire Protection Engineering

by

Elisa Schulz Baker

June 2011

APPROVED:

Professor Albert J. Simeoni, PhD., Major Advisor

Alexander Maranghides, Reader

Professor Kathy A. Notarianni, PhD., Head of Department

Abstract

The Wildland/Urban Interface, in which homes are intermingled with forested areas, presents unique challenges to fire protection and fire prediction, owing to the different fuel loads, conditions, and terrain. Computer models that predict fire spread through such an area require data for multiple scales, from crown fire spread to the heat release rates and ignition conditions for individual trees, as well as an understanding of fire behavior and spread. This discussion investigates a means by which fire behavior for Douglas-fir trees can be determined from quantifiable characteristics, such as height and moisture content. Mass, flame height, peak heat release rate, and total energy can be estimated from these simple measurements. A time scale of 60 seconds, combined with a peak heat release rate estimated from tree size characteristics, provides an approximation of total energy that is within 11% of measured values. Pre-heating of trees with a low (2.5 kW/m^2) radiant heat flux did not have a noticeable impact on the resulting heat release rate. In addition, fire spread between trees was highly dependent on the presence of ambient wind; in the absence of wind or wind-borne embers, the trees were very resistant to ignition even when in close proximity (3 spacing). With the addition of wind, the fire would spread, although the heat release rates were dramatically reduced for trees of sufficiently high moisture content ($< 70\%$).

Acknowledgements

I would like to thank the Fire Protection Department of WPI, who in 2002 approved an internship with NIST, and then in 2003 extended it for a year in order to allow me to continue with the fire tests and turn the experience into a thesis. Certainly many thanks to Kathy Notarianni, and Dave Lucht are owed. Also to Alex Maranghede for allowing me to assist with the tree burning tests, and serving as reader for this thesis. Thanks are due to John Woycheese, my initial advisor who had many great suggestions and editorial assistance, Professor Simeoni for stepping in to take over, and Kathy again for helping me to finish up, at long last.

Also many thanks to friends and family who have never ceased cheering me on.

Contents

1	Introduction	1
1.1	Chapter Descriptions	2
1.1.1	Tree Size Variation and Scaling of Data	3
1.1.2	Exposure to Radiant Heat Before Ignition	3
1.1.3	Fire Spread Amongst Closely Grouped Trees	4
2	Background Information	5
2.1	Previous Work Done	5
2.1.1	Heat Release Rate Studies	5
2.1.2	Flammability of Landscaping Plants	6
2.1.3	Radiant Pre-Heating	7
2.2	Review of the Current State of Fire Models	8
3	Tree Size Variation and Scaling of Data	11
3.1	Methodology	11
3.1.1	Instrumentation	12
3.1.2	Trees	14
3.1.3	Test Procedure	17
3.2	Results and Analysis	18
3.2.1	Moisture Content	18

3.2.2	Mass loss	23
3.2.3	HRR	26
3.2.4	Tree Mass as a Function of Height and Leaf Area	30
3.2.5	Imaging (Flame Characteristics)	34
3.2.6	Flame Temperatures	40
3.2.7	Heat Flux	43
3.2.8	Comparison Across Species	47
4	Exposure to Radiant Heat Before Ignition	50
4.1	Methodology	51
4.1.1	Instrumentation	51
4.1.2	Procedure	57
4.2	Results and Analysis	63
4.2.1	Moisture Content	64
4.2.2	Mass Loss	68
4.2.3	Heat Release Rates	69
4.2.4	Leaf Area	72
5	Fire Spread Amongst Closely Grouped Trees	76
5.1	Procedure	77
5.2	Results and Analysis	87
6	Uncertainty	90
6.1	Thermocouples	91
6.2	Heat Flux Gauges	91
6.3	Heat Release Rate	92
7	Conclusions	94

8 Future Work	97
8.1 Flux Time Product	98
A HRR Curves of Trees Exposed to Radiant Heat Flux	102
B Thermocouple Tree Data	103

List of Figures

3.1	Instrument layout showing positioning of thermocouples and heat flux gauges, where distance A is adjusted to place the thermocouples midway between tree trunk and outermost branches for each specimen. HFG7 is positioned at an angle of 20 degrees.	13
3.2	The crown height of a Douglas-fir tree is measured from the bole height, or bottommost branch, to the base of the top-most growth.	16
3.3	A photo of the Computrac Max-1000 sample pan with dehydrated Douglas-fir needles after the moisture content of a sample has been measured.	20
3.4	Peak HRR/mass from Douglas-fir trees as a function of moisture content showing the curve-fit line developed by Babrauskas and the data used in deriving it (circular data points), as well as data obtained during this study (triangular data points). Also shown are the three moisture content regimes – $MC < 30\%$, $30\% < MC < 70\%$ and $MC > 70\%$, indicated by vertical dashed lines.	22
3.5	The role of moisture content on the percentage of mass consumed showing how different regimes affect the percentage of mass consumed, with a linear curve fit overlaid on the data.	25

3.6	HRR plotted over time of the nine trees burned in the first phase of testing, from start to 120 seconds which encompasses the entire burn from ignition to flame-out.	27
3.7	HRR curves from the 9 trees burned in the first phase, aligned so that the peak HRR occurs along the same vertical axis, allowing a direct visual comparison of the rate of increase, which shows that the different sizes of trees all took approximately 30 seconds to reach peak HRR.	28
3.8	Triangle approximations for the heat release rate curve of a Douglas-fir tree created using the peak HRR and a 60 second time interval are shown overlaid on the actual HRR curve for 2 selected trees, 4-3 and 12-2.	29
3.9	This chart shows the agreement between the measured value of energy released, and the triangle approximation used to calculate heat released by means of the peak HRR and a 60 second duration.	30
3.10	A screenshot from the software program used to create and count colored pixel overlays which are used to calculate leaf area. In this example the pixels that meet criteria of color and hue matching those of the needles are highlighted and counted, allowing surface area to be measured for irregular-shaped objects such as trees.	32
3.11	Comparison of the relationships between crown height, leaf area and tree mass for use in estimating mass by means of a trendline from either leaf area or crown height data.	34
3.12	Fire video image-captures arranged by 5 second centered around the time of peak HRR showing the progression from ignition to peak is nearly the same time scale in all tree fires regardless of tree size.	35

3.13	Flame height graphic showing how the mean flame height was derived from analysis of digital photos. The thermocouple tree was used as a reference point, as each thermocouple was at a known height, and the mean flame height was the distance measured from the base of the fire to the top of the flame where intermittency was 0.5.	37
3.14	Flame height data showing relationship between crown height and the ratio of flame height to crown height which shows that trees will have flame heights between 1.5 to 3 times the crown height, depending on tree size.	39
3.15	Relationship between plume temperature measured at TC1 and peak HRR.	42
3.16	Peak temperatures measured at each thermocouple station, where TC1 is the highest thermocouple, and TC7 is the closest to the tree's base.	43
3.17	The peak incident heat fluxes recorded for all seven gauges which were located at positions oriented horizontally and vertically relative to the fire.	46
3.18	A plot showing the crown height and peak HRR for two different species of trees - the Douglas-fir trees tested in this study, and Scotch Pine trees which had been burned previously in a study on Christmas tree home ignition hazards.	48
4.1	Experimental setup for the tree burns after the trees have been exposed to radiant panels showing thermocouple tree and load cell located under hood.	52

4.2	Diagram of the heat flux gauges 1 through 3 at the platform under the calorimeter hood where the trees were burned, located 1 m, 2 m and 10 m from the tree center.	52
4.3	Diagram showing locations of the two heat flux gauges at the radiant panel; one in place behind the tree, and one next to the trunk of the tree.	53
4.4	Diagram showing locations of the two heat flux gauges in place behind the tree, and next to the trunk of the tree at the radiant panel. . . .	55
4.5	Labeling convention for tree faces used when photos were taken of all sides of the trees before the exposure to the radiant panel, and after the burn was completed.	57
4.6	This photo shows the gridded backdrop used for photos so that the area of the trees could be later measured using a computer software program.	58
4.7	Sampling points for the needles taken to measure moisture content are shown here. Samples were taken from the bottom, middle, and top thirds of the tree, labeled as points 1, 2 and 3, from the front and rear faces of the tree.	59
4.8	Plan view diagram of methane burner used for ignition of trees. . . .	61
4.9	Side profile diagram of gas burner used for ignition of trees, also showing the position of the tree relative to the burner when in place for ignition.	62
4.10	Photo of flames, reaching approximately 12 cm high, from the gas burner used to ignite trees.	63

4.11	Bar graph showing the measured moisture content from samples taken from the front middle section of the trees before and after exposure to the radiant panels for differing lengths of time.	65
4.12	The percentage drop in moisture content for 9 trees sampled in 6 different places - three on the side facing the radiant panel, and three on the far side. Samples taken from the back side of the tree showed negligible drops in moisture content.	67
4.13	HRR-time curve for a tree that has been exposed to radiant heat for 50 minutes and then ignited, showing the dual-peak phenomenon that some of the trees exhibited.	71
4.14	Photo a one of the trees prior to being burned in front of the grid backdrop used to calibrate distances in the digital photos for the purpose of measuring the leaf area, where the distance between 'A' and 'B' is known.	73
4.15	Chart showing the relationship between leaf area and tree mass for trees from both the first and second series of tests, which were obtained from different tree farms.	74
5.1	Experimental setup for fire spread experiments test 1; 4 trees spaced at 1 foot apart	78
5.2	Experimental setup for fire spread experiments test 2; two trees spaced at 3 in	79
5.3	Experimental setup for fire spread experiments test 3; tree spacing at 6 in with inclusion of fan at 3.15 m – diagram not to scale.	80
5.4	Experimental setup for fire spread experiments test 4; tree spacing at 6 in, fan at 7.42 m	81

5.5	Video capture from test 4 showing the flame angle due to wind as flames spread from tree #4 to tree #12.	82
5.6	Experimental setup for fire spread experiments test 5; tree spacing at 6 in, fan at 7.42 m	84
5.7	Experimental setup for fire spread experiments test 6 with a 2 MW heptane burner located next to 3 trees of high moisture content. . . .	85
5.8	Photo of heptane burner heating a cluster of trees as part of fire spread experiments.	86
5.9	Comparison of mass and peak HRR for the 4-foot trees burned in the first series, tree variation and scaling, and last series of tests, flame spread.	88
8.1	Flux-Time Integral (FTP) example showing the relationship between heat flux, FTP-ignition and predicted ignition time	100

List of Tables

3.1	Douglas-fir tree identification key; heights; and masses at time of purchase, after ten days, and immediately before ignition. The percent of mass left after moisture loss due to evaporation is presented in the final column.	17
3.2	Recorded values for all trees, including mass, peak HRR, mass loss and moisture content	26
3.3	Data table showing the tree heights, and the flame heights as calculated from digital photographs	40
3.4	Peak flame temperatures and the location they were measured, as well as the temperature measured at TC1 which was the highest thermocouple located 4.3 m above the tree base. Average temperature is the average of the peak temperatures recorded at each of the 7 thermocouples for a given test discounting those below the seat of the fire.	41
3.5	The peak values recorded at each of the seven radiant heat flux gauges are shown here for each tree burned.	44
3.6	Heat flux measurements, calculated total heat flux and radiative fraction.	47

4.1	Heat flux map created at different points in front of the radiant panels. Heat flux measurements were taken at 13 different heights along the centerline at .6 m distance and, and 3 additional measurements were taken, two 30 cm off-center, and one at .9 m distance.	56
4.2	The average moisture content from six sampling points of the trees after exposure to radiant heat flux for various durations of time. . . .	68
5.1	The peak HRRs for the trees burned as part of the test series on fire spread.	89

Chapter 1

Introduction

As land development continues and communities are established ever farther from urban centers, the encroachment of homes and other structures into areas that were previously forested complicates life safety and fire protection. The challenges presented by these mixed environments require greater understanding of the interplay between structures and forests and knowledge of how to estimate fire risk and prevent unwanted losses.

Different computer models that incorporate the physics of fire and empirical data of fire behavior can predict the path a fire will take through a structure or home, or the spread of a forest fire through acres of land. The two types of fire spread are very dissimilar. Forest fires spread through areas in which the fuel load can be considered a continuous bed, whereas structure fires are inherently concentrated, isolated loads. Where the two environments merge, known as the Wildland/Urban Interface (WUI), landscaping vegetation is more common than dense woods and undergrowth and the impact on housing from non-continuous vegetation, ignited by wildfire, bears investigation. Based on current national maps and statistics, 42 million homes in the US, or 37% of the nation's total, are located in the WUI [23],

which refers both to areas where housing adjoins heavily vegetated areas (interface) and those where houses and vegetation are intermingled (intermix).

In recent years, interest in wildland fires has increased, following several large, costly fires. In 2003, 4 of the 46 large-loss fires as reported by the NFPA were wildfires, causing a combined loss of 2126 million dollars. The two largest WUI fires, both in California, accounted for 73.8% of the total losses for the year [6]. In total, more than 10,000 homes and 20,000 other structures have been lost to wildland fires since 1970, according to the NFPA [7].

Although trees and shrubs that are located in the WUI can, if ignited, endanger adjacent structures, very little quantitative information exists about the ignition and burning characteristics of landscape vegetation. Generally, experiments conducted to measure the Heat Release Rate (HRR) of individual trees have assessed the hazards of Christmas tree fires [24, 4, 11]. Little information exists to quantify how HRR, burn duration, and flame height vary with the size of a tree or tree species, although two studies [17, 12] have explored the burning characteristics of shrubs.

Owing to their availability, widespread growing habits across the United States, and the existing literature, this study focused on Douglas-fir trees. The Douglas-fir, *Pseudotsuga menziesii*, is not a true fir – although it has needles similar to a fir tree – but is more akin to a type of Hemlock, the Japanese Tsuga (hence the genus *Pseudotsuga*). It grows over most of western North America and is quite common due to its hardiness, drought resistance and shade tolerance.

1.1 Chapter Descriptions

Three distinct test series were conducted over 14 months in the Large Fire Laboratory on the Gaithersburg, MD campus of the National Institute of Science and

Technology (NIST). The tests provided data on how tree size impacts fire characteristics, how pre-heating of a tree influences the burning, and the likelihood of fire spread among closely grouped trees in the presence or absence of wind or a large radiative source.

1.1.1 Tree Size Variation and Scaling of Data

To better understand and predict the behavior of fires in a WUI, computer models can evaluate the contributions of different weather conditions, fuel loads and spacing, and terrain aspects. These models, however, require data from burning of individual trees, among other inputs. Full-scale testing is cost-prohibitive to determine empirical model inputs for the myriad tree species and sizes. At present, there is no known methodology for scaling fire characteristics with tree size to extrapolate fire behavior for various tree sizes from a subset of data. The first chapter explores the impact of tree size on characteristics such as the maximum Heat Release Rate (HRR), the mass loss (burning) rate, and the total heat released. These will be related to measurable tree size variables: height, mass, and leaf area. Additionally, flame height, temperature, and radiative heat flux may determine how a burning tree will affect a nearby structure. A series of fully instrumented, full-scale burns in a laboratory with different size trees under free burn conditions will identify relationships that can scale key fire characteristics based on tree size. This information can be used in the development of fire spread models for the WUI.

1.1.2 Exposure to Radiant Heat Before Ignition

The next chapter addresses the effect of encroaching wildfire on landscaping vegetation. The radiant heat flux from a large flame front to the plants would dehydrate them as it raises their temperature, possibly leading to ignition from lower-energy

sources, or larger fires. Douglas-fir trees, the same species as were used in the previous section on scaling data, were subjected to pre-heating from a radiant panel. This panel exposed the trees to a constant incident heat flux of 2.5 kW/m^2 for 6, 25, and 50 minutes to determine the effect of radiant heating on overall flammability. Additionally, these tests were intended to quantify the incident heat flux required to affect time to ignition, peak HRR and total heat released, mass loss rate, and flame temperatures and size.

1.1.3 Fire Spread Amongst Closely Grouped Trees

The last chapter of the paper investigates flame spread amongst trees that are in close proximity to each other to determine the hazard posed by having trees planted close to one another under different levels of moisture content (such as well-watered plants or very dehydrated foliage), both in the absence and presence of wind. In addition, fire spread due to intense heating from a nearby pool fire was investigated.

Chapter 2

Background Information

2.1 Previous Work Done

2.1.1 Heat Release Rate Studies

There have been few experimental studies that investigated the heat release rates of individual trees. One study [24] measured the HRR of dry Scotch Pine trees under the instrumented hood in the large fire laboratory at NIST. A similar study by Babrauskas [4, 5] investigated Douglas-fir trees. Both studies involved only one tree height.

The Scotch Pine testing focused on the risks from over-dry Christmas trees in the home, probable ignition sources, and fire growth. Eight trees were tested, seven of which were air-dried 3 weeks after they were harvested; the eighth was kept in a tree stand full of water at all times. The trees were 2.5 to 3.1 meters tall, however it is not known what points the height was measured from. The dried trees were ignited via an electric match and had peak heat release rates from 1600kW to 5100kW. The eighth tree did not ignite. Moisture content measurements were taken from the trunk of the trees using a wood probe.

The study by Babrauskas, et al. [4, 5], also focused on Christmas trees in the home; a larger number of Douglas-fir trees were burned over the course of testing. Moisture content was investigated in depth by measuring the rate of water loss from fresh cut trees that are left to dry or displayed in water. It was found that a tree that is kept out of water will dry quickly until the stomata (minute pores on the needle or leaf surface through which gaseous interchange takes place) close after which time drying slows. Below a species-specific moisture content irreversible damage to cellular structure prevents a tree from rehydrating even if placed in water.

Babrauskas conducted a series of tests to determine the HRR hazard of trees displayed in homes. The tests were in a mock room with a ceiling and 2 walls forming a corner to simulate the typical placement of a Christmas tree in a home. The trees were, on average, 1.98m tall. 48 trees were burned following a period of 10 days display time, during which the level of care and watering was varied, to determine the effect of moisture content on HRR. As ignition, the trees weighed 6.4 kg to 22.4 kg, which was dependent on the moisture level of the trees. The moisture content at the time of testing was determined by sampling branches.

Trees with a moisture content of 50% or lower ignited from the application of a small flame to a branch. Trees that did not ignite were subjected to a 100 kW fire from a wrapped gift placed under the tree. The study showed a clear relationship between increasing moisture content and decreasing HRR. Excessively dry trees (below 15% moisture content) had HRRs in the range of 2000kW to 3000 kW.

2.1.2 Flammability of Landscaping Plants

In addition to trees, some studies have investigated the fire performance of landscaping plants. Typically, these studies center around flammability characteristics of plants at differing levels of dehydration stress to determine which are the most

resistant to fire spread and which pose the greatest hazard in the event of the WUI fire. As indicated in one Master's Thesis from the Wood Science and Technology division of UC Berkeley, a 1m^3 *Juniperous* bush with 60% moisture content had a peak HRR of approximately 1000 kW [12].

2.1.3 Radiant Pre-Heating

Prior to ignition, landscaping vegetation is pre-heated via radiant and convective heat transfer from the approaching flame front during a WUI fire incident. In a typical forest fire however, most of the convective energy rises in the plume, and does not impact the landscaping trees until the flame front is very close. Exceptions include high wind situations or sloped terrain. The amount of radiant heat flux that will be seen by landscaping vegetation, however, is a function of the configuration factor, which itself is based on distance, angle of sight, and dimensions of the landscaping and flame front.

Pre-heating evaporates moisture from the vegetation and raises the temperature of the plants. Additionally, the plant may be altered on a biochemical level by the preheating, releasing pyrolysates. These changes can increase the flammability of a plant and may decrease the time to ignition. When an ignition source, such as ground fire or flaming brand is proximate to a plant which has been preheated, it will be more easily ignited than one which has not been exposed to any preheating.

For an exposure duration of 60 seconds, which is how long individual Douglas-fir trees burned, an incident heat flux of $30\text{kW}/\text{m}^2$ would cause piloted ignition of a house with wood siding [14]. The minimum required heat flux for piloted ignition of Douglas-fir plywood is $13.1\text{kW}/\text{m}^2$ [1], and most wood siding requires 12 to 13 kW/m^2 , however for an exposure of only one minute a much higher flux is required (See 8.1 in Future Work for more discussion).

A series of tests were conducted in 1998, known as the International Crown Fire Modeling Experiment (ICFME) which sought to determine the home-ignition threat from a high-intensity crown fire located 10, 20, or 30 meters from a wooden house. As such, wooden sections of wall located at those distances from a large crown fire test were set up with heat flux gauges to record the incident heat flux. In the worst-case scenario tested here, the incident heat flux was 30kW/m^2 with the flame front at a distance of 28m [10]. For an actively burning (and therefore moving) crown fire, the flame front exposes a specific location for a duration on the order of 1 minute.

2.2 Review of the Current State of Fire Models

Wildfires are a natural part of the lifecycle of functioning ecosystems that can significantly affect human populations. Fire size; intensity; location; and the native plants, animals, and human interests are all factors that can affect whether a wildfire will be judged beneficial or not. A moderate fire can recycle nutrients to the soil, clear away choking underbrush, provide stimuli essential to the propagation of some fire-dependent species, and be easily contained or controlled. However, too large a fire can sterilize soil, preventing re-growth, and can be almost impossible to contain or control using current firefighting methods. There is a delicate balance in deciding what course of action to take when a wildfire is spotted, or a prescribed burn is planned – weighing the needs of the ecosystem against the possible costs when isolated homes or entire communities may be placed at risk. In some cases, a relatively benign fire from an ecological standpoint can be disastrous from a human one. Policy makers rely on up-to-date information on weather conditions, relative humidity levels, land contours, and other factors to aid their decisions. Fire models contribute predictions of fire growth based on a variety of input parameters.

Firefighter tactics and community evacuations may be adjusted based on these predictions. Other models analyze geographic information and weather patterns to determine the likelihood of a large destructive fire for a specific area of interest. A third, simplified, model helps informed homeowners evaluate the level of risk that different landscaping vegetation arrangements may pose to their properties.

Rothermel's Fire Spread Model (1972) was one of the pioneering fire models and still forms the basis for many physics-based models [22]. It is based on fundamental principles of combustion, supplemented with experimental work. The model, which predicted rate of spread of a flaming front, treats fire spread as a series of ignitions; therefore, fire growth is a ratio of heat received to heat required for ignition. The inputs include fuel properties, such as density and specific heat, fuel array arrangement; and environmental variables, such as wind velocity, slope and fuel moisture content.

EcoSmart was developed by the Center for Urban Forest Research at UC Davis, and is a model used to help landowners plan for better energy efficiency, water conservation, and fire safety. It is composed of several subsections, including FIRE-WISE, which estimates the risk of fire spread to a structure from nearby trees and other landscape vegetation. Version 1.0 incorporates a method to estimate the risk from fires through ignition by radiant heating. Other subsections include sub-models for hydrology, energy and economics.

FARSITE, or Fire Area Simulator, simulates the spread and behavior of wildland fires using a geographic information system (GIS) to provide data for fuels, elevation, slope, topographic aspect, and canopy cover. Outputs include fire size, intensity, rate of spread and heat release per unit area. Additionally, FARSITE includes spotting and crown fire routines and supports graphic display of the input data and calculations.

BEHAVE Fire Modeling System is a collection of interacting fire behavior modules. Typical inputs include terrain information, fuel parameters, and weather, and the outputs can predict containment time and final fire size, the probability of ignition, spotting distance, scorch height and rate of spread. Additionally, it is being expanded to include transition to crown fire, smoke production, and soil heating, as well as more extensive fuel characterization [26].

The previous models listed, while all are physics-based, are more empirical models based on experiments and observed behaviors coupled with trending and statistical analysis. Computational Fluid Dynamics (CFD) models are a recent development which bring numerical modeling to the field of WUI fire models. WUI Fire Dynamics Simulator (WFDS) will extend the capabilities of the Fire Dynamics Simulator (FDS) time-based three-dimensional structure fire model developed at NIST to include outdoor fire spread and smoke transport problems [19]. Similarly, FIRETEC which was first developed in 1997 [18] as a wildfire physics models has been coupled with an atmospheric fluid dynamics model (HIGRAD) to numerically model heat transfer, mass and momentum transport, turbulence and combustion [9]. These models bring a great deal to the table in terms of predicting WUI fires as they are refined and expanded, but the tradeoff comes in increased computational resources needed, data requirements, and longer runtimes.

Chapter 3

Tree Size Variation and Scaling of Data

The first series of tests were designed to determine if the heat release rates and other fire characteristics can be scaled for different sized trees of the same species. Multiple trees of three different heights (4-foot, 8-foot and 12-foot) were selected from a tree farm and burned under the same conditions. From analysis of this data, fire sizes for other heights can be interpolated.

3.1 Methodology

The trees were burned in the Large Fire Laboratory located at the National Institute of Standards and Technology (NIST) campus in Gaithersburg, Maryland. The facility has several instrumented hoods that employ oxygen consumption calorimetry to measure HRR. The largest hood calorimeter, which was used for the tree burns, has a HRR capacity of approximately 15 MW and measures 9 m \times 12 m. The lower edge of the hood is 4.5 m above the floor level and the center of the hood is 7.9 m

above the floor. In addition to the HRR, the mass loss, plume temperature, and radiative heat flux were recorded during the tests.

3.1.1 Instrumentation

The trees and their stands were placed on a platform supported by a load cell (LC1) that recorded the mass loss as a function of time. A much larger platform was placed underneath the first (see Figure 3.1) to catch any falling partially-consumed material and was supported by load cells at each of the four corners (LC2), the readings from which were totalled.

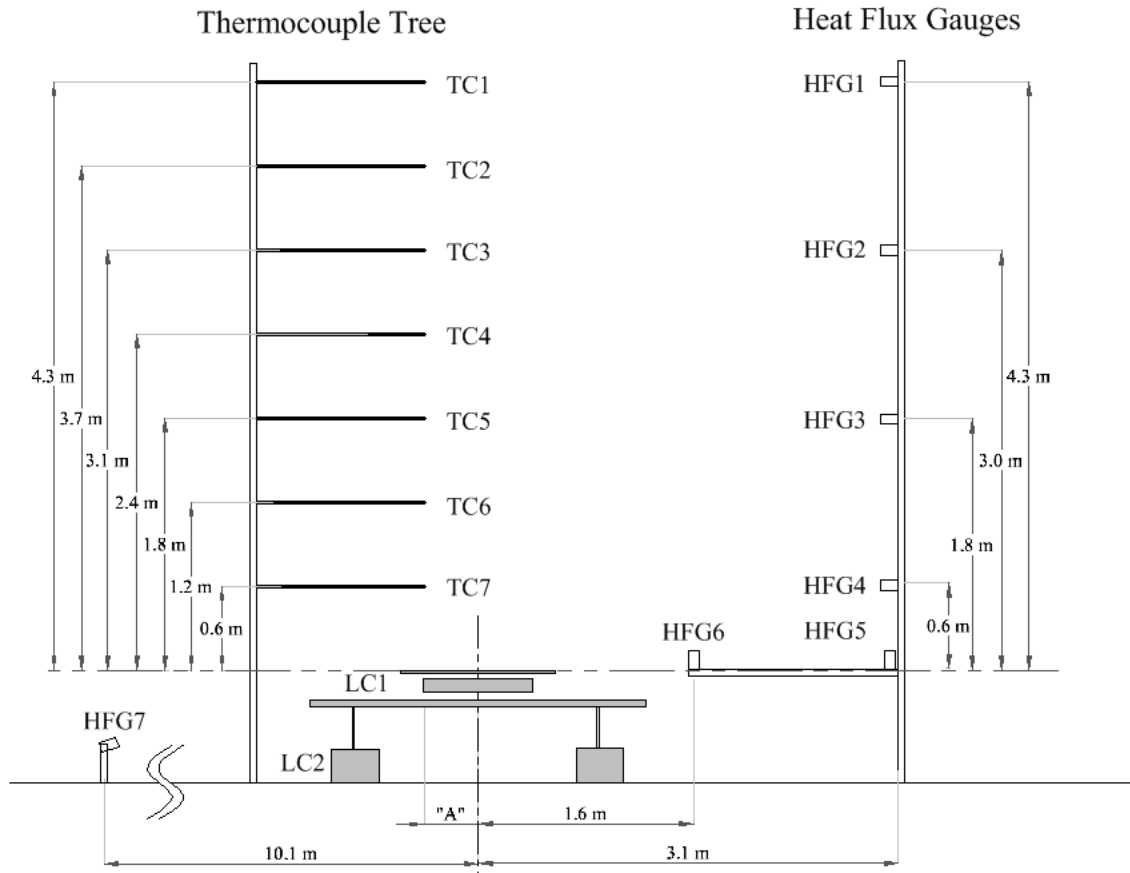


Figure 3.1: Instrument layout showing positioning of thermocouples and heat flux gauges, where distance A is adjusted to place the thermocouples midway between tree trunk and outermost branches for each specimen. HFG7 is positioned at an angle of 20 degrees.

Seven thermocouples were mounted every 0.61m (2 ft) above the tree platform up to 4.2 m (14 ft) on a vertical thermocouple tree. The thermocouple tree was shifted for each test to place the thermocouple beads midway between the trunk and the outermost branches. The 3 mm diameter sheathed thermocouples were 0.91m (3 ft) long, and had an exposed bead. Voltage output from the thermocouple

array was recorded on the Large Fire Laboratory data acquisition system.

The first three tests had 6 heat flux gauges in place, 4 of which were mounted on a 4.3 m (14 ft) vertical support located 3 m (10 ft) along the horizontal axis from the trunk of the trees. The first gauge was 0.6 m (2 ft) above the tree platform, and the remaining gauges were spaced vertically every 1.2 m (4 ft). The remaining two heat flux gauges (HFG5 and HFG6 as show in Figure 3.1) were mounted at platform level, facing upward 1.5 m (5 ft) and 3 m (10 ft) from the trunk. For the fourth through ninth tests, a seventh heat flux gauge was added, 10 m (32.8 ft) away from the tree trunk at ground level, angled at 20 degrees to view the entire flame.

During each burn the experiments were videotaped from three perspectives, and digital still photographs were taken.

3.1.2 Trees

Three nominal tree heights were selected for the experiments. The maximum height of the trees was limited by the HRR capacity of the exhaust hood. The Douglas-fir trees were purchased from a local farm that grows Christmas trees. Three trees each with commercial sale heights of 1.2 m, 2.4 m, and 3.7 m (4 ft, 8 ft, and 12 ft, respectively) were cut on July 6, 2003. These trees were delivered to NIST the following day, weighed and tagged. The tree designations throughout the report are based on their commercial height, i.e. 4-1 refers to the first 4 ft tree burned.

For conditioning purposes, the trees were stored on open racks outdoors in a way that permitted airflow around the entire tree to dry them in an even manner to drought-like conditions. The racks were covered by tarps to shield the trees from rain. After 10 days, the trees were brought inside and weighed again to monitor the moisture lost to evaporation. They were dried for 7 more days inside the Large Fire Laboratory where the mass loss was monitored. Some of the tree trunks were

trimmed to create a level base for attachment to a 4 ft \times 4 ft plywood board, used to hold them upright during the testing.

The trees were photographed and heights were measured (see Table 3.1). The crown height, H_c , is the distance from the bole (the location on the trunk of the first live branch off the trunk) to the base of the top branch as shown in Figure 3.2. This differs from the commercial height of the tree, which is typically measured from the ground to the tip of the stem. The crown height is a more accurate representation of the burnable mass, eliminating the top stem and base of the tree up to the bole height. The former can extend 0.3 m above the highest branch but has negligible mass and makes no significant contribution to the total heat released, and the tree trunk typically chars, contributing little additional energy release. The needles and small branches are the primary fuel load for an evergreen tree.

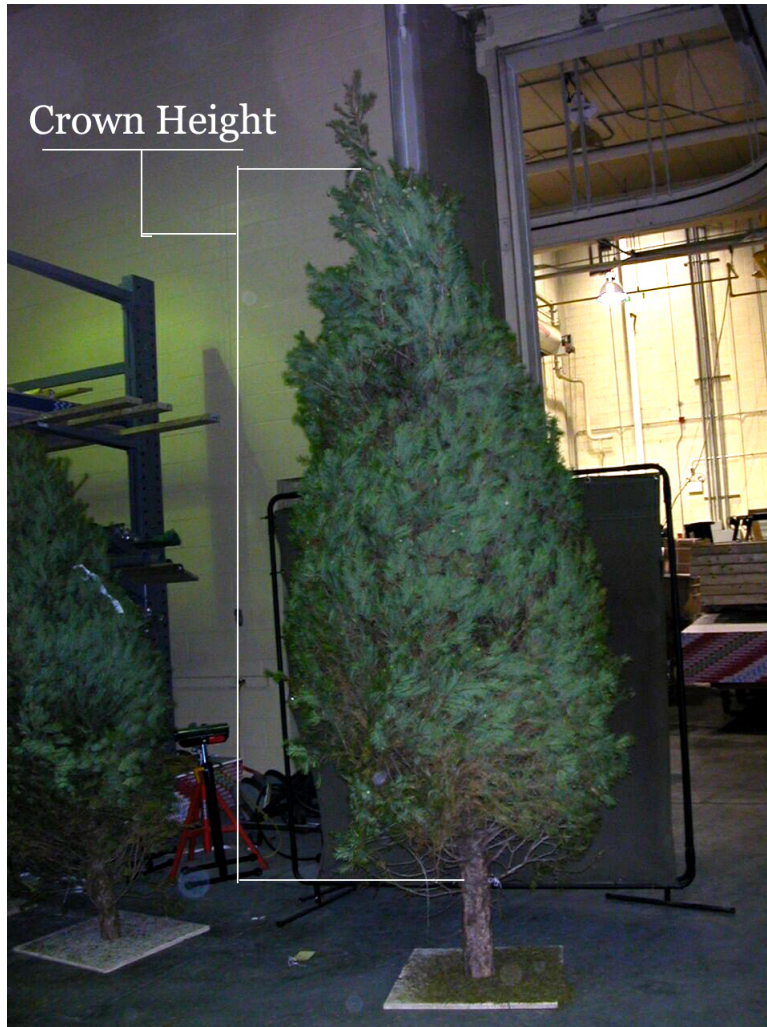


Figure 3.2: The crown height of a Douglas-fir tree is measured from the bole height, or bottommost branch, to the base of the top-most growth.

The final mass after drying for 17 to 21 days was recorded and divided by the initial mass to determine how much moisture was lost to evaporation. The smaller trees lost approximately 50% of their mass whereas the larger trees lost, on average, 25-30%, as seen in Table 3.1, below.

Table 3.1: Douglas-fir tree identification key; heights; and masses at time of purchase, after ten days, and immediately before ignition. The percent of mass left after moisture loss due to evaporation is presented in the final column.

Tree	Test No.	Crown Height (m)	Bole Height (m)	Total Height (m)	Weight 7/7/03 (kg)	Weight 7/17/03 (kg)	Weight Pre-burn (kg)	% original mass at time of test
4-1	Test 1	1.37	0.08	1.45	5.16	3.01	2.85	0.55
4-2	Test 4	1.30	0.19	1.49	3.54	1.61	1.55	0.44
4-3	Test 7	1.42	0.22	1.64	8.4	4.52	4.37	0.52
8-1	Test 2	2.31	0.27	2.58	23.1	17.6	17.6	0.76
8-2	Test 5	2.62	0.43	3.05	24.4	18.1	17.6	0.72
8-3	Test 8	2.44	0.48	2.92	40.8	29.6	28.8	0.70
12-1	Test 3	3.10	0.69	3.78	38.2	30.1	29.9	0.78
12-2	Test 9	3.20	0.71	3.91	41.3	33.1	31.9	0.77
12-3	Test 6	3.33	0.50	3.82	38.3	29.3	29.1	0.76

3.1.3 Test Procedure

The tests were conducted over a span of 5 days. The trees were set on the load cell platform and needle samples (3 - 5 clippings) were taken from the ends of the branches located in the middle third of the tree height. The samples were sealed in individual zip-lock bags and a lightproof container and frozen for later analysis (see section 3.2.1 for more details).

After the tree had been sampled and weighed, it was ignited at the base of the crown with a propane torch. The torch was Y-shaped with two flames approximately 1 foot apart for simultaneous ignition points on opposite sides of the trunk. Depending on the moisture content, some trees required only 5 seconds of torch application to ignite, whereas others required 10 to 15 seconds before they could sustain burning on their own. The means and relative ease of ignition of the trees is a topic of interest for future research, but for the purpose of these tests sustained burning was required. The trees were allowed to burn to completion, during which time the

HRR, mass loss, flame temperature, heat flux and visual images were recorded.

3.2 Results and Analysis

This section will delve into the results obtained from the instrumentation in place, as well subsequent analysis performed on the data and images.

3.2.1 Moisture Content

The moisture content of fuel is the primary factor that determines whether a fuel package will ignite with a given heat source. Correlations between fuel moisture content and ease of ignition, likelihood of spotting and general burning conditions were compiled by Albin [3], who used relative humidity as a surrogate for fine fuel moisture content, such as that of needles from an evergreen. Fuels with moisture contents under 15% are described as being susceptible to all sources of ignition; in the range of 15-30% they can be ignited with a match and will have a rapid buildup, and 40-60% requires a larger ignition source, such as that of a campfire. When fuel moisture content reaches >60% the chances of ignition are very low.

When ignition does occur, the moisture content of available fuel plays a critical role in fire behavior, including time to ignition, fuel consumption rate, intensity and smoke production [22]. Moisture content is typically expressed on a dry basis using the following equation:

$$MC = \frac{M_{wet} - M_{dry}}{M_{dry}} * 100\% \quad (3.1)$$

M_{wet} and M_{dry} are the mass of needles when they are fresh and after they have been oven-dried to evaporate all moisture, respectively. A well-watered and healthy tree will have a moisture content in excess of 100%.

At the time of testing in July 2003, there was no oven available to measure the

MC of the collected samples. For this reason, the samples were sealed in air-tight, light-proof containers and frozen for 12 months, at which time an Arizona Instruments Computrac Max-1000 moisture analyzer was used to analyze all samples.

The Computrac is a self-contained analyzer with a scale, sample pan, and heating element that was programmed for Douglas-fir test parameters as determined by forestry scientists. The sample pan with some needles after testing can be seen in Figure 3.3. It takes an initial reading of a sample's mass, and then gradually heats up the sample to a temperature of 165°C, as this is a temperature at which moisture is lost without significant damage to the cellular structure of the plant. The ending criterion is a rate of moisture loss of less than 0.200% per min. Samples sizes of 3.0 g \pm 2.0 g were used.



Figure 3.3: A photo of the Computrac Max-1000 sample pan with dehydrated Douglas-fir needles after the moisture content of a sample has been measured.

Although there is a level of uncertainty associated with the moisture content data after a year of cold storage, the results are comparable to predicted values based on previously published data. In an extensive study of Douglas-fir Christmas trees, Babrauskas developed an empirical correlation of peak HRR/mass and moisture content of the needles. This curve-fit was published in the SFPE Handbook [4] as follows:

$$\frac{\dot{q}_{peak}}{m} = e^{5.84-0.017M} \quad (3.2)$$

Where \dot{q}_{peak} is the peak heat release rate (kW), m is the total pre-burn mass of the tree (kg), and M is the moisture of the needles (percent by weight).

The data for the curve-fit equation is based on averaged moisture contents from samples taken at both inner and outer branches; samples for this study were taken only from outer branches. Figure 3.4 compares Babrauskas' data using both the averaged moisture content values and those taken from outer branches only, to that obtained from this series of tests. The moisture content and HRR/mass data obtained here fits reasonably well within the spread of data points, lending confidence to the values of moisture content obtained from the frozen samples.

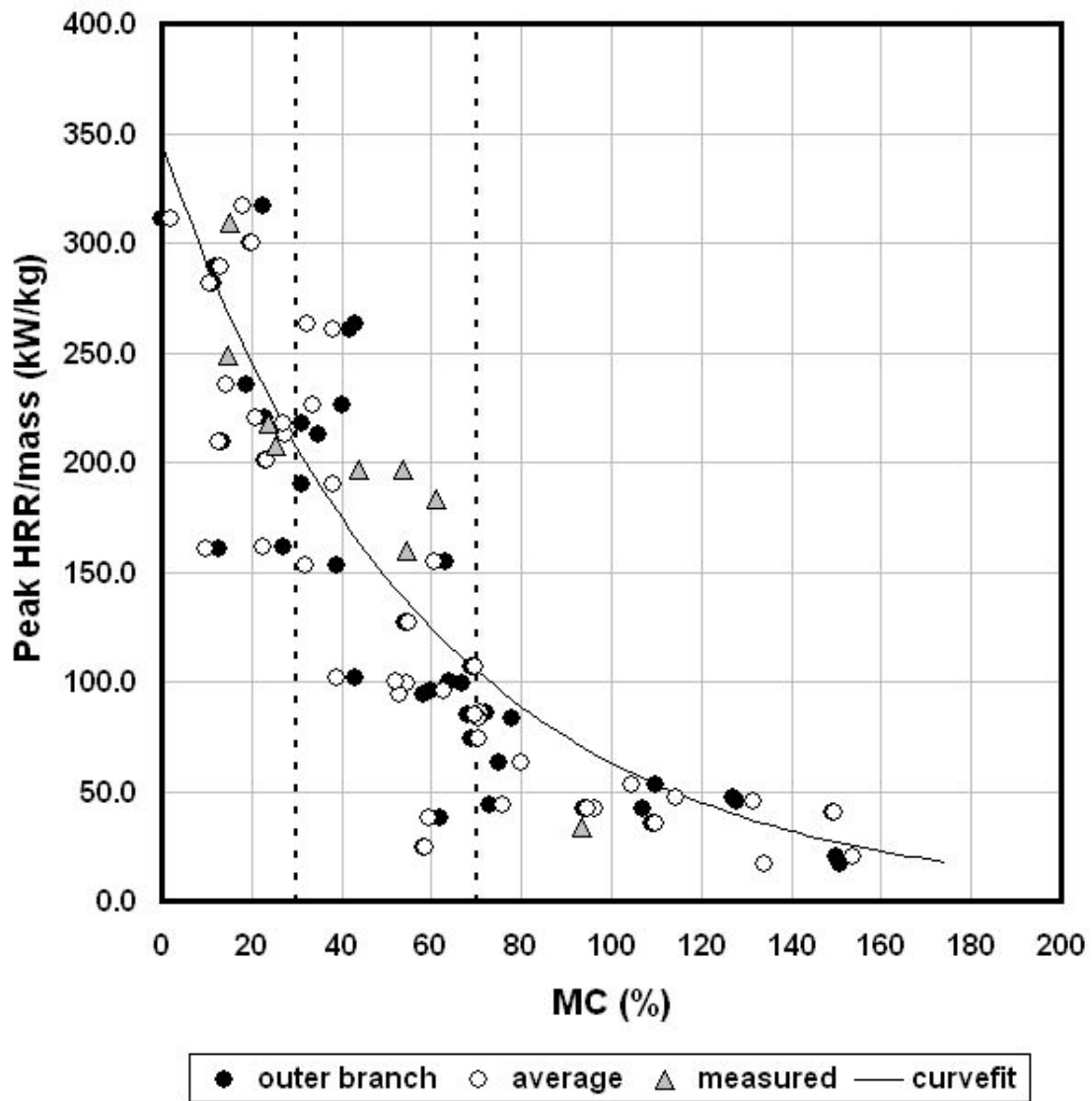


Figure 3.4: Peak HRR/mass from Douglas-fir trees as a function of moisture content showing the curve-fit line developed by Babrauskas and the data used in deriving it (circular data points), as well as data obtained during this study (triangular data points). Also shown are the three moisture content regimes – $MC < 30\%$, $30\% < MC < 70\%$ and $MC > 70\%$, indicated by vertical dashed lines.

The moisture content analyses are also in agreement with previous research done

by Chastagner, who found that Douglas-fir trees with a moisture content of 30% or less will be fully consumed, those with a moisture content of 30-70% are in the transition range where the tree will likely be partially consumed if successfully ignited, and trees with >70% moisture content will not sustain burning [5]. The trees tested in this study are divided into these three regimes, $MC < 30\%$, $30\% < MC < 70\%$ and $MC > 70\%$, with regime 1 being the most dry and regime 3 being too wet to sustain burning. These regimes are also indicated in Figure 3.4 by the vertical dashed lines.

Tree 12-1 (the third tree burned) was visually much more green than the other trees, due to its relatively high moisture content (regime 3), and exhibited different combustion behavior from the other eight trees. It was never fully involved and large portions remained unburned after the test. Because it could not sustain burning, the results for that test are not included in segments of the analysis that are based on complete consumption of the needles. However, this burning pattern is indicative of what would be expected from trees that have not been excessively dried before testing or have not experienced a severe drought condition, and the comparatively low peak HRR for a tree of that size fits well with the curve-fit line mentioned previously.

3.2.2 Mass loss

The trees lost an average of 50% of their pre-burn mass during the combustion phase; the moisture content determined how completely a tree would burn. Figure 3.5 shows the effect of the moisture content of the needles on the mass loss, although it is not a precise means of predicting burned mass. The percentage of mass consumed was calculated by dividing the total mass lost (as reported by the load cells) by the total initial mass, which necessarily includes the tree trunk. However, the trunk does

not contribute significantly to the mass loss, as it forms char and resists burning. By far, needles and small stems represent the bulk of mass lost, although this is not quantified. Based on a visual analysis of the trees post-burn, 90-100% of the needles are consumed when the tree is very dry, i.e., in MC regime 1. This loosely correlates to 50-60% of the total mass, but is dependent on a particular tree's ratio of burnable mass (needles) to unburnable mass (trunk).

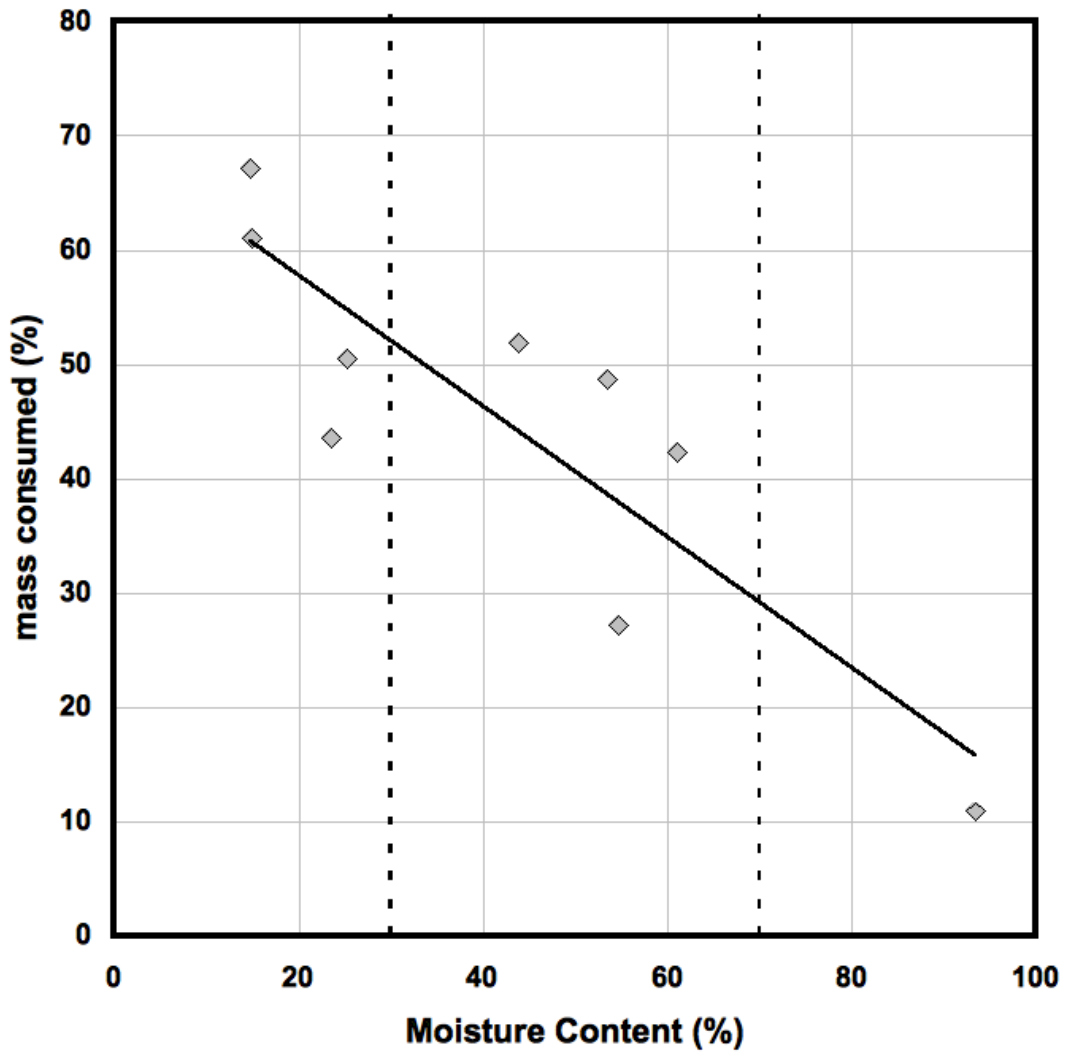


Figure 3.5: The role of moisture content on the percentage of mass consumed showing how different regimes affect the percentage of mass consumed, with a linear curve fit overlaid on the data.

Table 3.2: Recorded values for all trees, including mass, peak HRR, mass loss and moisture content

Tree	HRR_{peak} (kW)	Tree Weight Pre-burn (kg)	Mass Loss (kg)	Mass Consumed (%)	Moisture Content (%)	MC Regime
4-1	778	2.85	1.44	51	25.21	1
4-2	719	1.549	1.04	67	14.75	1
4-3	1661	4.372	2.67	61	15.01	1
8-1	3347	17.6	9.13	51	43.87	2
8-2	3402	17.64	8.6	49	53.57	2
8-3	5035	28.75	12.53	44	23.57	1
12-1	855	29.92	3.265	11	93.42	3
12-2	4976	31.92	13.49	42	61.00	2
12-3	4007	29.14	7.91	27	54.61	2

3.2.3 HRR

Figure 3.6 provides a plot of the measured HRR curve for each of the trees burned. For some of the trees, there was a significant delay between the start of the test when the ignition source was applied, and established burning, leading to a staggered appearance of the curves. Established burning is defined as the time at which the fire starts to rapidly grow towards its peak and an ignition source is not needed. Based on this definition, trees in moisture content regime 1 reached established burning in 1 to 7 seconds whereas trees in regime 2 and 3 required a longer growth period of 8 to 27 seconds.

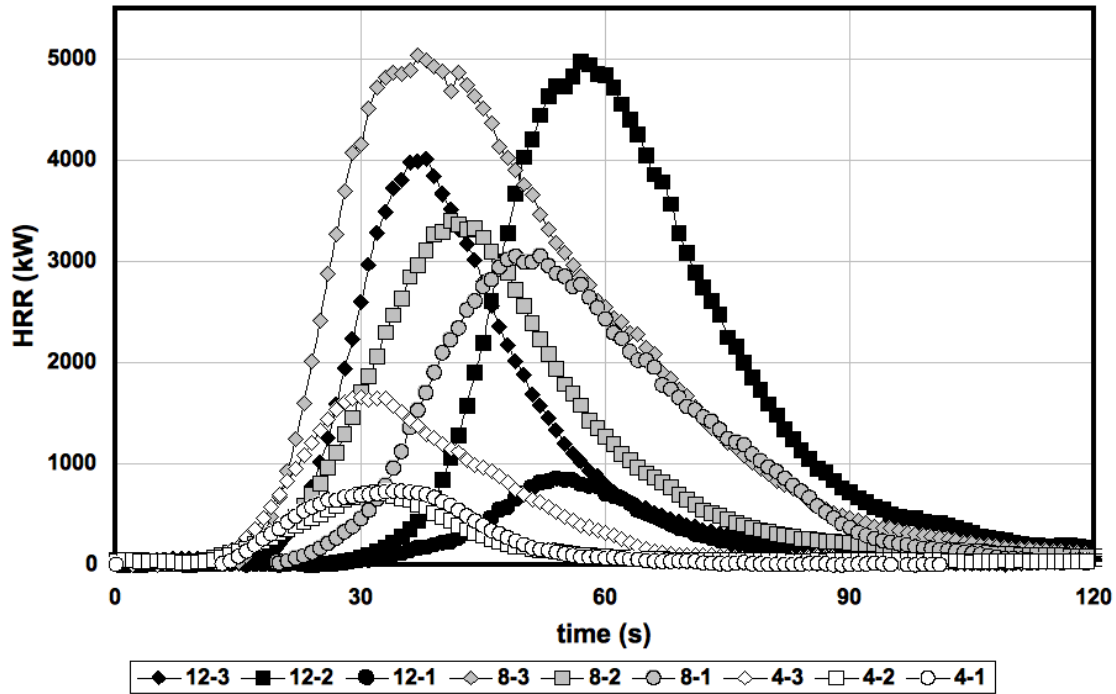


Figure 3.6: HRR plotted over time of the nine trees burned in the first phase of testing, from start to 120 seconds which encompasses the entire burn from ignition to flame-out.

The experiments demonstrated that there is a similarity in the shape of the HRR curves from start to peak HRR among all the trees. All trees required approximately 30 seconds to reach peak HRR from established burning, regardless of height or mass. Figure shows the HRR curves transposed to align the peak HRR at 30 seconds. From this figure, it is apparent that the size of the tree plays a large role in determining the peak HRR for the dry trees, but has a negligible effect on the total burn time. Tree 12-1 was the exception to this general rule, as its peak HRR was comparable to that of the 4 foot trees. However, this is to be expected due to its unusually high moisture content (93%) relative to the other trees, placing it into moisture content

regime 3.

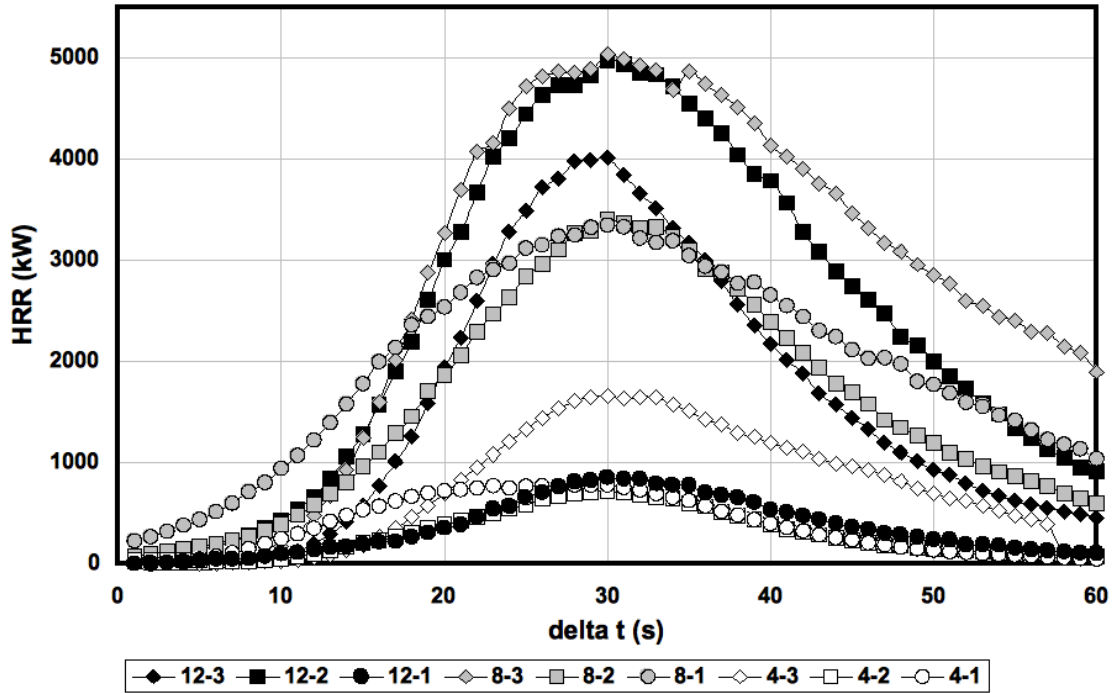


Figure 3.7: HRR curves from the 9 trees burned in the first phase, aligned so that the peak HRR occurs along the same vertical axis, allowing a direct visual comparison of the rate of increase, which shows that the different sizes of trees all took approximately 30 seconds to reach peak HRR.

Using 60 seconds as a common time interval for burning, the total heat released by the Douglas-fir trees can be approximated by a triangle, as demonstrated in Figure 3.8 for two of the measured HRR curves. The area of the triangle ($0.5 \cdot 60 \text{ s} \cdot \text{peak HRR}$) compares favorably to the actual area under the measured HRR curve (total energy released in kJ), as seen in Figure 3.9. Although more testing is required to determine if other tree species can be approximated in this manner, the methodology does provide a simple way to determine the total heat released during

the burning of individual Douglas-fir trees. The moisture content and mass of a given tree can predict the peak HRR using the relationship given in Equation 3.2.

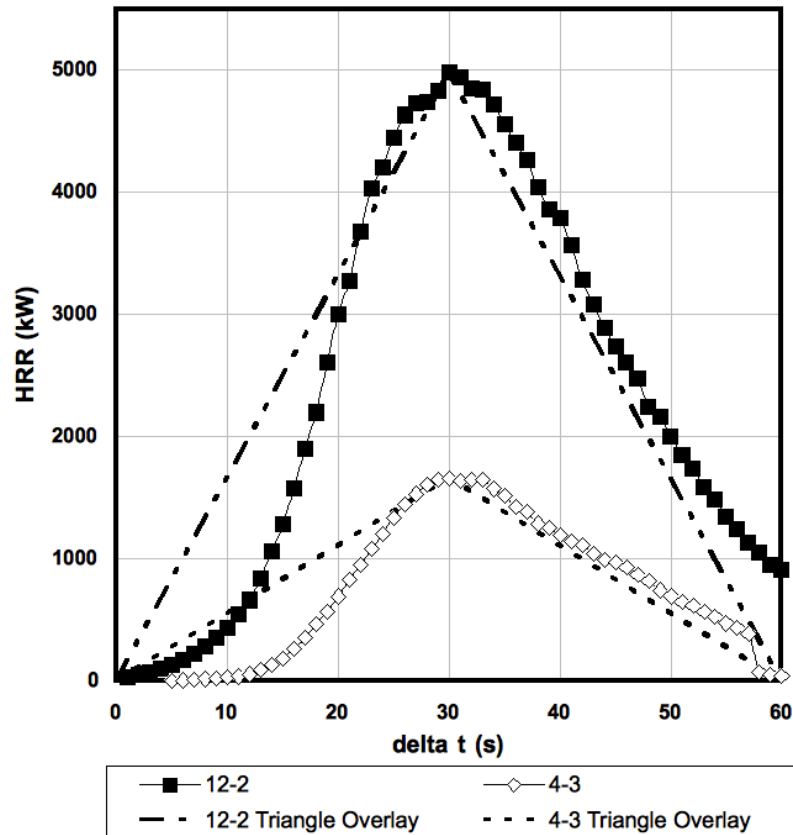


Figure 3.8: Triangle approximations for the heat release rate curve of a Douglas-fir tree created using the peak HRR and a 60 second time interval are shown overlaid on the actual HRR curve for 2 selected trees, 4-3 and 12-2.

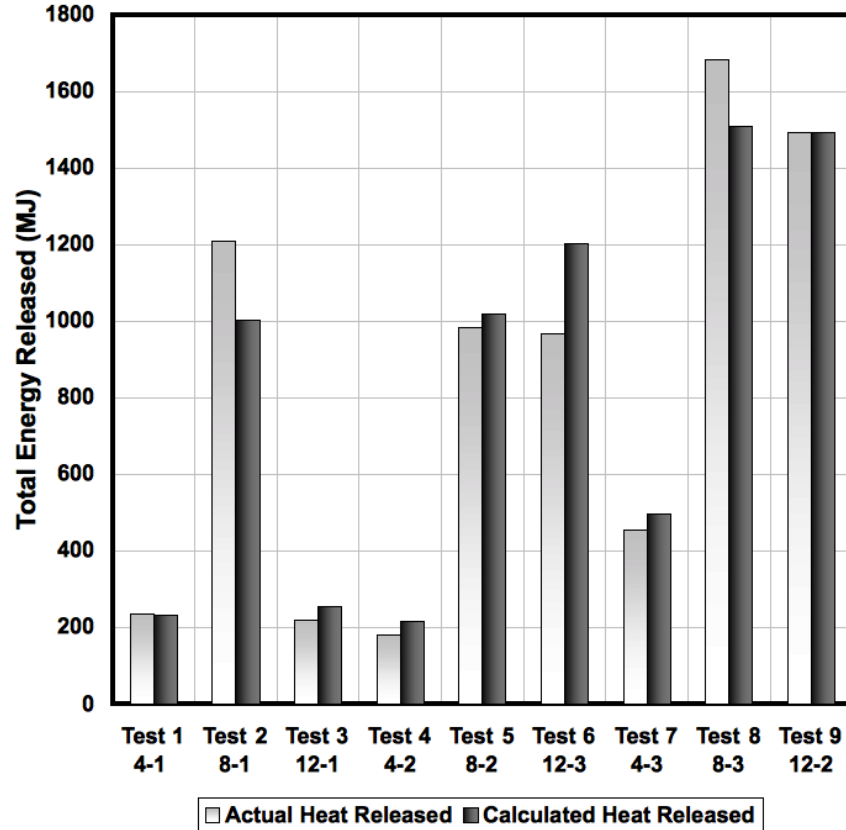


Figure 3.9: This chart shows the agreement between the measured value of energy released, and the triangle approximation used to calculate heat released by means of the peak HRR and a 60 second duration.

3.2.4 Tree Mass as a Function of Height and Leaf Area

To predict the peak HRR and total heat released of Douglas-fir trees by means of Equation 3.2 and the triangle approximation the mass must be known or estimated. The mass is a function of the tree’s age and trunk diameter, the density of the needle growth, height and moisture content; as such, mass can be difficult to estimate for trees that have not been harvested. A preliminary methodology to estimate tree mass uses the tree’s crown height (as detailed in section 3.1.2). This simplistic

approach relies on the relatively uniform axis-symmetric shape of Douglas-fir trees. For trees with uneven growth patterns and deciduous trees, a more rigorous approach will be needed.

Calculating mass from leaf area may be viable across a wider range of tree species. Leaf area is a measure of the surface area of a tree's crown occupied by leaves or needles and is utilized to predict a tree's behavior in such areas as pollution interception, rainfall storage and CO₂ sequestering [20]. The trunk and large branches do not play a large role in individual tree fires; therefore the leaf area is a logical indicator of burnable mass and fire size. Another commonly used measure is the surface area to volume ratio, or σ , which defines the density of foliage and can describe how flammable a plant may be, in conjunction with moisture content [27].

To determine the leaf area of a tree, digital images and a data analysis software package were utilized. The software used was Sigma Scan Pro, which allows a user to measure the area of irregular objects from digital photographs by creating a colored overlay that maps to individual pixels that match your criteria of intensity and/or hue, as shown in Figure 3.10. The program then counts how many pixels are covered by the overlay. It is possible to calibrate the photo using a known or measured distance and a two-point rescaling, which translates the distance on the photo measured in pixels to the user-supplied actual distance and units. The measured tree crown heights were used for this calibration purpose, and the area was converted from total pixels to square meters.



Figure 3.10: A screenshot from the software program used to create and count colored pixel overlays which are used to calculate leaf area. In this example the pixels that meet criteria of color and hue matching those of the needles are highlighted and counted, allowing surface area to be measured for irregular-shaped objects such as trees.

Figure 3.10 illustrates the overlay applied to tree 4-1 to measure the area of

needles from a photo. In the given example, 199768 pixels were counted, which translates to 0.583 m². The tree has a crown height of 1.37 m, which is equal to 806.8 pixels in the original picture, giving a calibration factor of 0.1709, or 100 pixels = 0.1709 m. In order to translate a sum of pixels to square meters the following equation is used:

$$Area = pixels * \frac{0.17^2}{100} \quad (3.3)$$

The area was obtained in this manner two times for each tree burned, from two photos taken 90° relative to one another, and then averaged, which should account for any lopsided trees.

A comparison of the two methods for estimating mass, leaf area and crown height, in Figure 3.11 shows that using the leaf area as a means of predicting mass has a slightly higher R² value than using the crown height (0.91 vs. 0.87)¹. Using the leaf area method of estimating mass also has potential applicability to other species, and for this reason would be recommended over using the tree height for future applications. However, in the case of the Douglas-fir trees tested in this study, the leaf area method tends to over predict mass, which in turn leads to higher than measured peak HRR predictions.

¹An R² value, also known as the coefficient of determination, is a number from 0 to 1 used to indicate how closely a trendline corresponds to the data it is created from, where 1 would indicate perfect agreement between data points and a trendline.

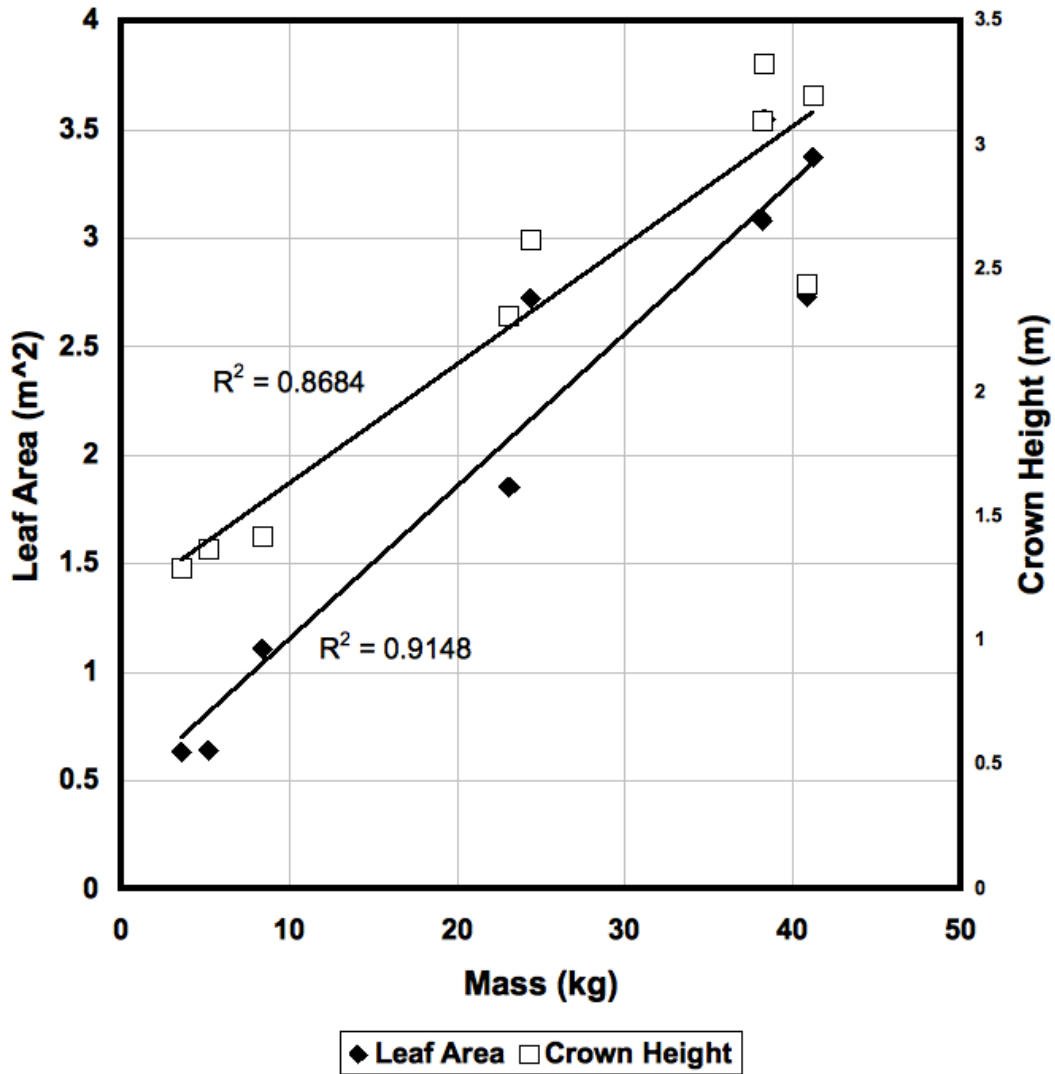


Figure 3.11: Comparison of the relationships between crown height, leaf area and tree mass for use in estimating mass by means of a trendline from either leaf area or crown height data.

3.2.5 Imaging (Flame Characteristics)

Figure 3.12 presents a timeline of images captures at five-second intervals centered on the time of the peak HRR. The fire growth rate visible in the stills taken from

video recordings of the experiments (tree 12-2 was not taped) shows the similar times to peak HRR from ignition, as was indicated in Figure 3.7.



Figure 3.12: Fire video image-captures arranged by 5 second centered around the time of peak HRR showing the progression from ignition to peak is nearly the same time scale in all tree fires regardless of tree size.

The mean flame height, H_{flame} , was determined for each experiment by analyzing video and still photos showing the burning tree, using the thermocouple tree as a reference. The flame height (see Figure 3.13) is the distance from the base of the flame near the tree bole to the top of the flame where the flame intermittency is 0.5, at which height the flame is visible 50% of the time. Still photographs were used to determine the flame height, in conjunction with the video record showing flame intermittency. In the case of this study, the mean flame height, H_{flame} , differs

slightly from the flame height L that is common in the literature, in that included in the height is the burning fuel package. It is difficult to provide direct comparisons to flame height calculations that are based on the flame height above the fuel, which is in many cases a gaseous diffusion flame, or crib fire. To model a fire's impact on its surroundings in the WUI, it makes little sense to disregard the flaming portion of the tree and focus only on the flame extending above it; however, if a value for L is needed, it would merely be the flame height H_{flame} minus the crown height H_{crown} .

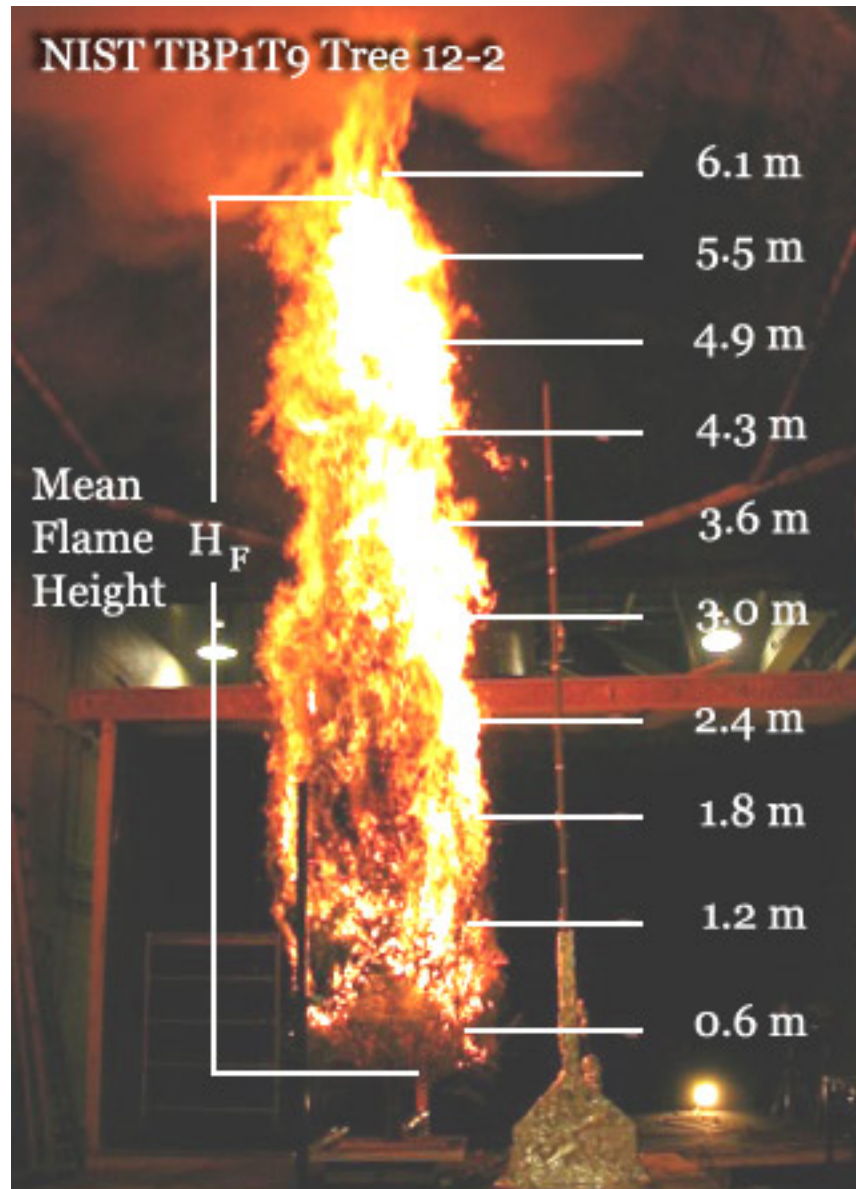


Figure 3.13: Flame height graphic showing how the mean flame height was derived from analysis of digital photos. The thermocouple tree was used as a reference point, as each thermocouple was at a known height, and the mean flame height was the distance measured from the base of the fire to the top of the flame where intermittency was 0.5.

A linear relationship was found between the crown height and the ratio of the flame and crown heights, with the largest ratios resulting from the smallest trees (see Figure 3.14). Depending on tree size, the flames were, on average, twice the height of the tree crown. Trees with a crown between 1 and 1.5 meters, however, will have a mean flame height that is roughly three times that. Predicting flame height, in conjunction with a flame temperature, enables calculation of the radiative heat flux to which a nearby structure may be exposed.

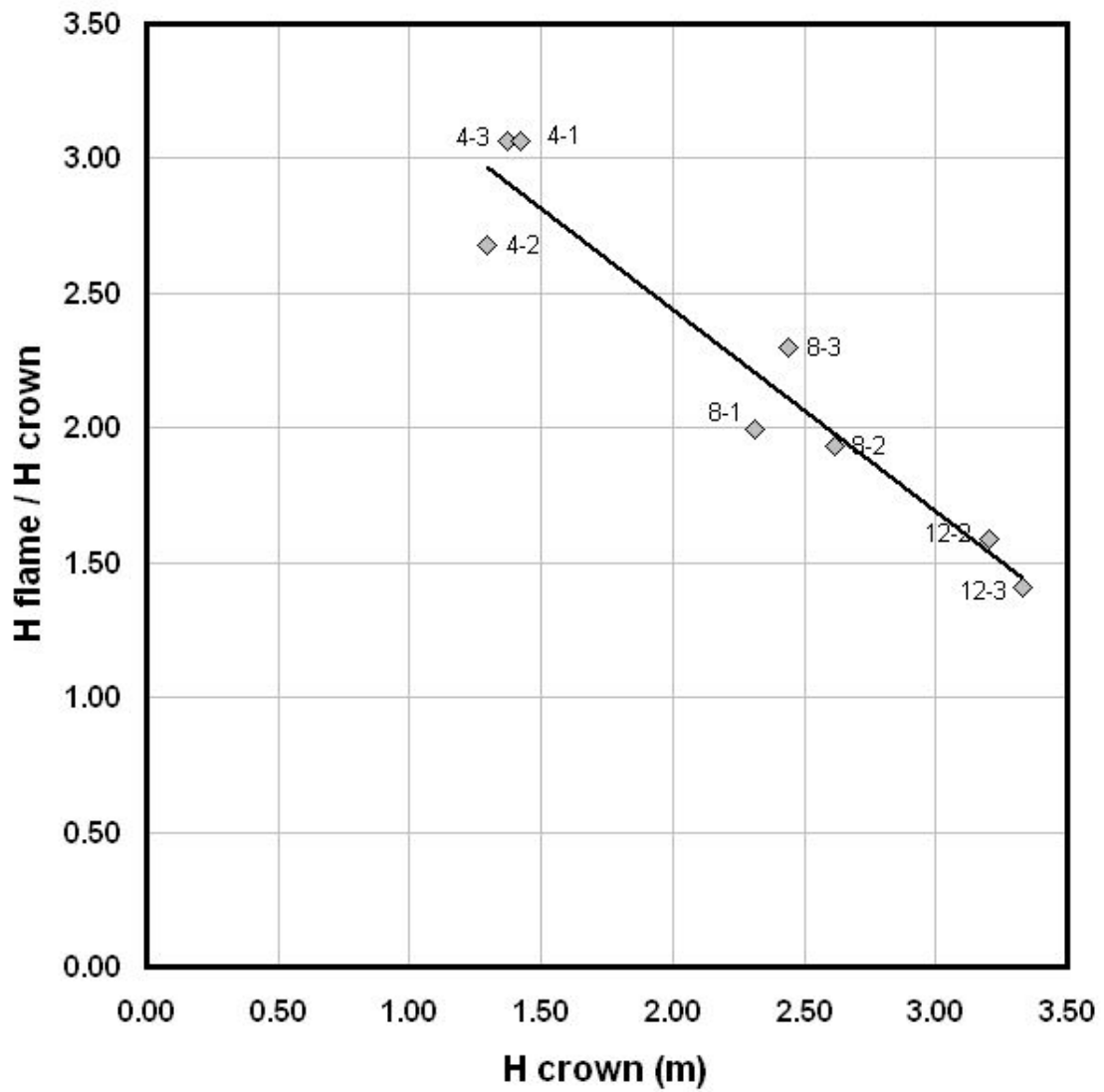


Figure 3.14: Flame height data showing relationship between crown height and the ratio of flame height to crown height which shows that trees will have flame heights between 1.5 to 3 times the crown height, depending on tree size.

Table 3.3: Data table showing the tree heights, and the flame heights as calculated from digital photographs

Tree	H_{crown} (m)	Flame Heigh(m)
4-1	1.3716	4.2
4-2	1.2954	3.47
4-3	1.4224	4.36
8-1	2.3114	4.61
8-2	2.6162	5.05
8-3	2.4384	5.61
12-1	3.0988	N/A
12-2	3.2004	5.08
12-3	3.3274	4.69

3.2.6 Flame Temperatures

The temperature of the fire and plume was measured via seven thermocouples from 0.6 to 4.3 meters above the tree base. The peak temperatures were usually measured by either TC6 or TC7, which are the lowest two thermocouples, located 0.6 and 1.2 m above the tree base, respectively. This is the height at which the tree has the most needles and is also at its widest, which leads to a higher volume of dead needle and twig material in the interior of the tree. Table 3.4 shows the recorded peak values and locations as well as the measured temperature at the highest thermocouple, TC1.

Table 3.4: Peak flame temperatures and the location they were measured, as well as the temperature measured at TC1 which was the highest thermocouple located 4.3 m above the tree base. Average temperature is the average of the peak temperatures recorded at each of the 7 thermocouples for a given test discounting those below the seat of the fire.

Tree	Peak Temp (C)	Location of Peak	TC1 (C)	Average (C)
4-1	803	TC6	117	402
4-2	730	TC7	226	535
4-3	910	TC7	246	554
8-1	1010	TC6	409	674
8-2	914	TC6	449	675
8-3	997	TC6	598	776
12-1	458	TC2	366	337
12-2	967	TC5	572	744
12-3	677	TC5	448	525

The plume temperature can be characterized by TC1, which at a height of 4.3 meters was well above the areas of intense burning on even the tallest trees. It is difficult to pinpoint the base of the fire, as it varied from tree to tree, but it was typically at or around the lowest thermocouple, TC7 at 0.6 meters. That would make the plume temperature as measured by TC1 at the height of 3.7 meters above the seat of burning. If Tree 12-1, which did not fully ignite, is discounted, a clear relationship between peak HRR and plume temperatures can be seen in Figure 3.15.

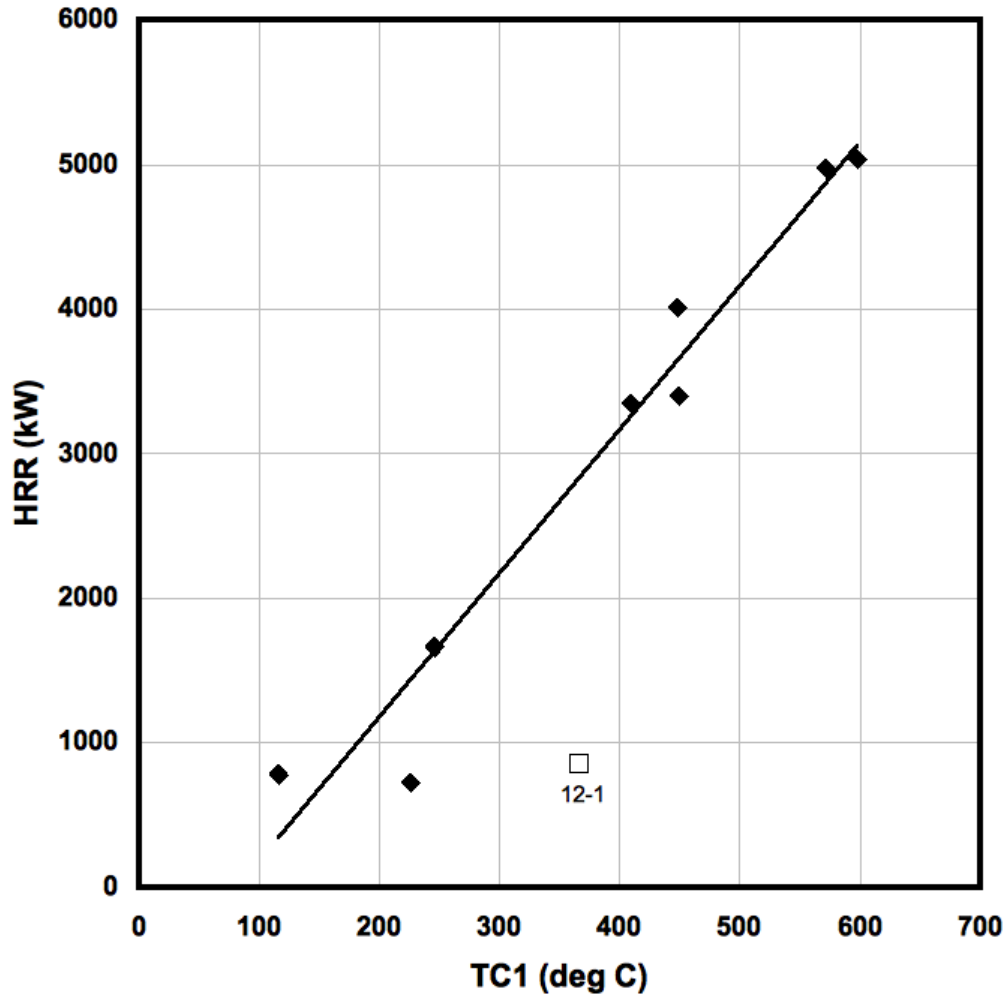


Figure 3.15: Relationship between plume temperature measured at TC1 and peak HRR.

The lower thermocouples record higher temperatures, as would be expected due to cold air entrainment into the higher sections of the plume. However, in the case of the 8- and 12-foot trees the lower thermocouples are below the seat of the fire and, as such, register a lower temperature (see Figure 3.16). The average value of the peak measured temperatures, which might be used to characterize the fire,

is presented in Table 3.4. The averages do not include the temperatures recorded below the seat of the fire.

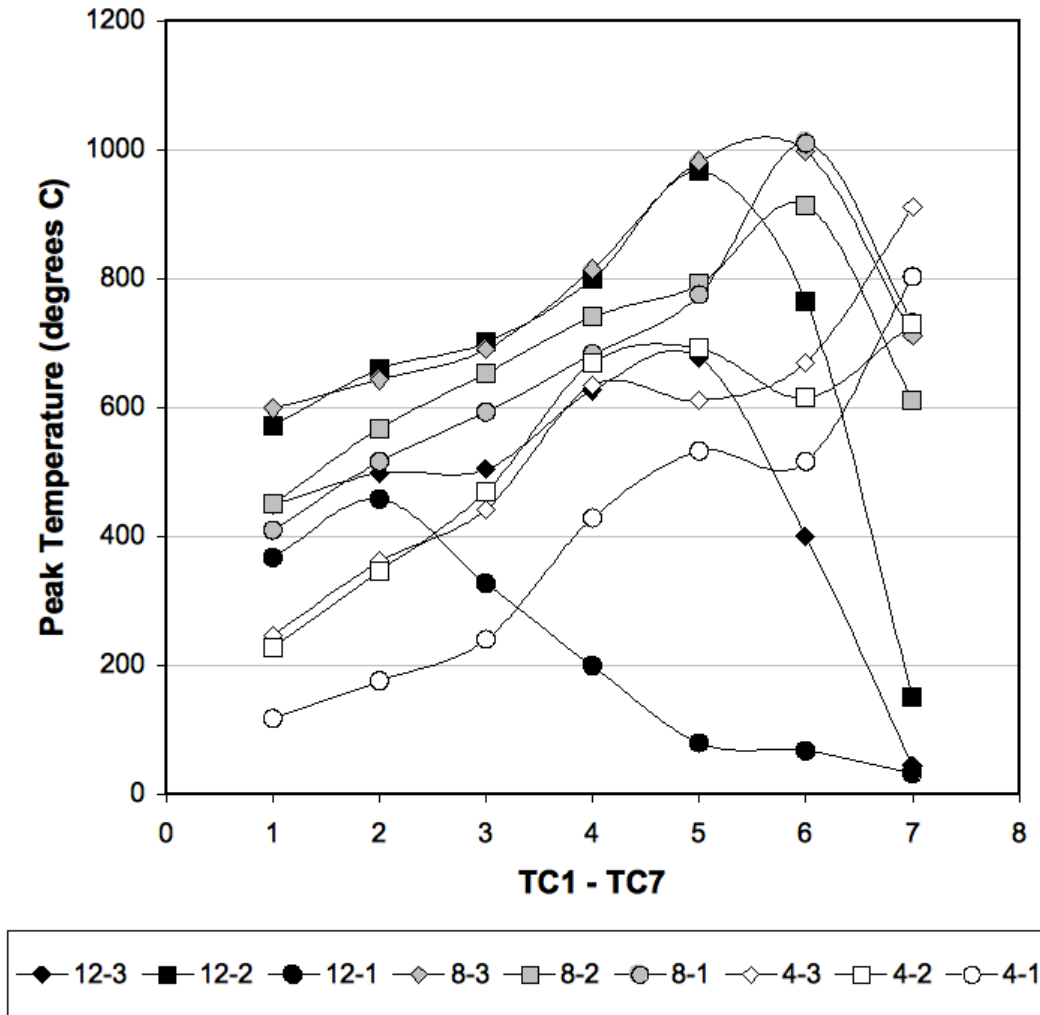


Figure 3.16: Peak temperatures measured at each thermocouple station, where TC1 is the highest thermocouple, and TC7 is the closest to the tree's base.

3.2.7 Heat Flux

Structure ignition in a WUI zone can result from any of several sources, such as burning brands (airborne embers that can be lofted a great distance ahead of a

flame front), convective heating (when a flame or fire plume actually impinges upon a structure), or radiative heat transfer. Although radiation from a single burning tree to a nearby structure is not likely to cause ignition, it can still enhance fire spread by pre-heating the structure, which lays the groundwork for ignition from an airborne brand.

For the first two tests (4-1 and 8-1), six heat flux gauges were in place to measure the incident flux within 3 meters of the burning tree. Starting with test 3, a seventh heat flux gauge was added at a distance of 10m from the trees to capture total radiation. The measured peak incident heat flux values for all seven gauges are shown in Table 3.5. Referring back to Figure 3.1, the arrangement is such that gauges 1 through 4 were arranged vertically at a distance of 3.1 meters from the centerline of the tree, at different heights. Gauge 1 was 4.3 meters above the tree base, and gauge 4 was 0.6 meters above the base. Gauges 5 and 6 faced upwards at ground level 1.6 and 3.1 meters from the tree centerline to record the heat flux experienced by grasses or shrubs in the vicinity of the tree. Gauge 7 was located at a distance of 10 meters.

Table 3.5: The peak values recorded at each of the seven radiant heat flux gauges are shown here for each tree burned.

	Gauge 1	Gauge 2	Gauge 3	Gauge 4	Gauge 5	Gauge 6	Gauge 7
Tree	kW/m ²						
4-1	1.26	1.62	2.04	1.98	0.80	1.88	N/A
4-2	1.14	1.38	1.76	1.69	0.72	1.71	0.17
4-3	3.82	4.60	4.81	4.33	2.08	3.96	0.50
8-1	4.12	4.96	5.55	5.08	2.54	5.21	N/A
8-2	4.54	5.12	5.72	4.88	2.58	5.14	0.55
8-3	9.21	9.21	8.68	7.44	4.27	7.65	0.00
12-1	1.64	1.88	1.74	1.06	0.70	0.78	0.11
12-2	5.88	6.56	6.45	4.66	2.93	3.79	-0.01
12-3	4.91	5.09	4.73	3.39	2.35	3.49	0.50

To predict heat flux from a burning tree, characteristics of the flame itself are needed: height, diameter and temperature. Flame height is a function of tree height and moisture content, and the width is fairly constant. Once the dimensions and temperature of a flame are known, the radiation from the flame can be calculated to predict the flux from a single burning tree to a nearby structure. By treating the flame as a 2-dimensional rectangle oriented towards a large receiver, such as a wall, the incident flux can be calculated by using Equation 3.4.

$$q'' = F \cdot \epsilon \cdot \sigma \cdot T_f^4 \quad (3.4)$$

where q'' is the incident heat flux in (kW/m²), F is the view factor, ϵ is the flame emissivity, σ Stefan-Boltzman constant (K⁴kW/m²), and T is the flame temperature (K). Assuming an emissivity of one and treating the flame as a black-body emitter will produce the most conservative estimates. The view factor, or configuration factor, takes into account the distance and orientation of the receiver with regards to the emitter.

As an example, for tree 8-2, which has a flame height of 5 m and a width of 0.8 m (both determined using the scaling technique shown in 3.13), the configuration factor to calculate radiation from a rectangle to a parallel small element of surface dA works out to be 0.096. Using the average flame temperature of 675 C, or 948 K, the incident heat flux is calculated to be 4.4 kW/m² at the height of 2.7 meters, which corresponds most closely to heat flux gauge 3, which recorded 5.72 kW/m². However, if the temperature recorded at thermocouple 5 (791°C) is used instead of the average temperature, the result increases to 6.9 kW/m². The appropriate value is likely between these results. TC5 represents the temperature at the very dry needles in the center of the fire plume and not the gas temperature at the boundary of the flames, which would be lower due to entrained air. This is one

of the limitations of using a 2-dimensional rectangle to model heat flux: choosing an appropriate flame temperature (This issue remains when modeling the flame as a cylinder.) As an initial attempt to predict the incident heat flux with known or estimated values of temperature and dimension, the two-dimensional model provides a rough estimate.

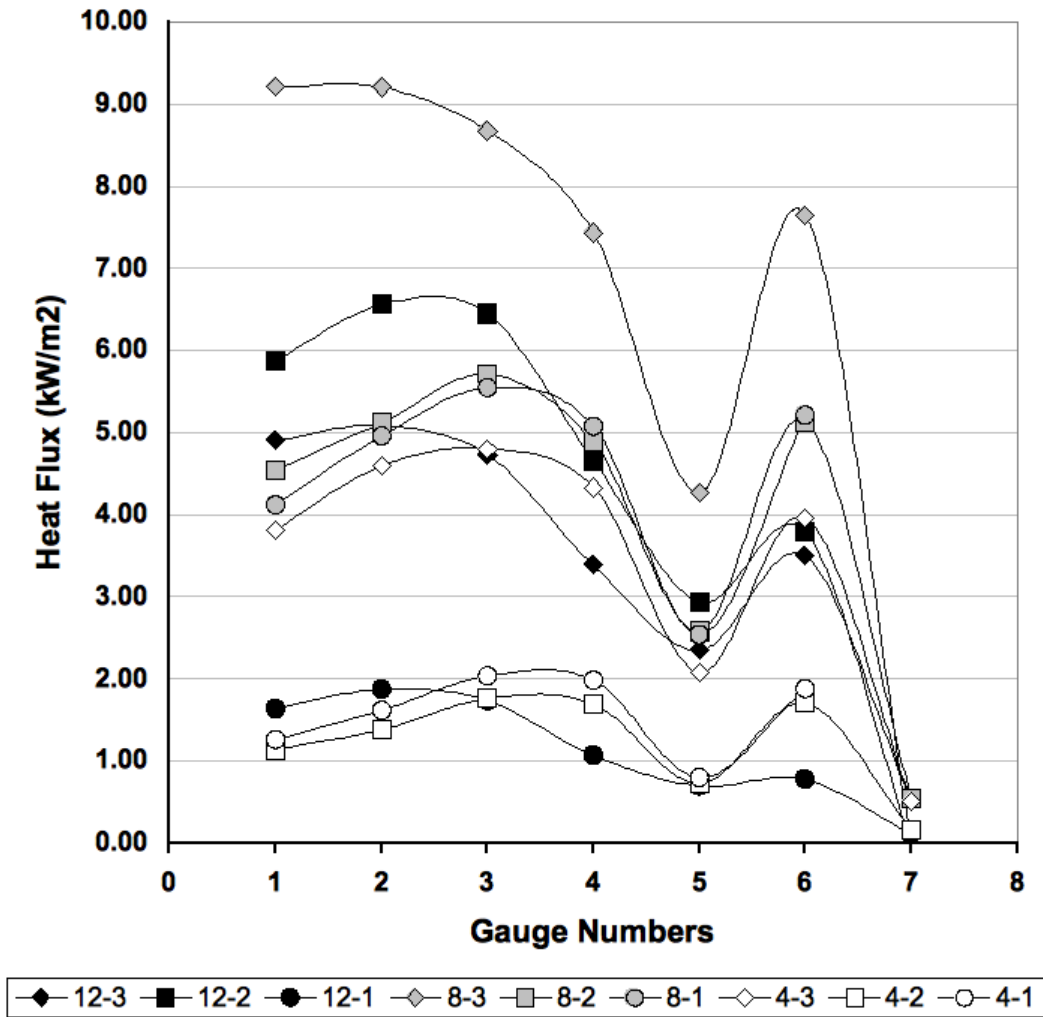


Figure 3.17: The peak incident heat fluxes recorded for all seven gauges which were located at positions oriented horizontally and vertically relative to the fire.

To measure the total flux, the remote heat flux gauge was able to see most of the flame, as opposed to the gauges located 1m away from the burning tree. Treating the flame as a point source, total flux was calculated for a sphere, so the measured heat flux was multiplied by $4\pi r^2$. The heat flux was measured 10 meters from the base of the tree, the distance r was calculated from the gauge to the tip of the tree, which approximately corresponds to center of the total flame (see section 3.2.5). These results, along with the peak HRR and calculated contribution to the total heat released are shown in Table 6. Only four tests of the six had uncorrupted data.

Table 3.6: Heat flux measurements, calculated total heat flux and radiative fraction.

Tree	H_{crown} (m)	Peak HRR (kW)	Peak Flux (kW)	Radiative Fraction (%)
4-2	1.30	720	220	30
4-3	1.42	1660	670	40
8-2	2.62	3400	771	23
12-3	3.33	4000	760	19

3.2.8 Comparison Across Species

There is a dearth of similar tests involving different species but there is some data available from seven individual Scotch Pine tree burns which were conducted at NIST [24] (an eighth tree did not ignite). These experiments were conducted in a laboratory setting, although the trees were burned in a room-corner configuration, which would likely lead to slightly higher HRRs due to re-radiation from the corners. The two sets of data were plotted together in Figure 3.18.

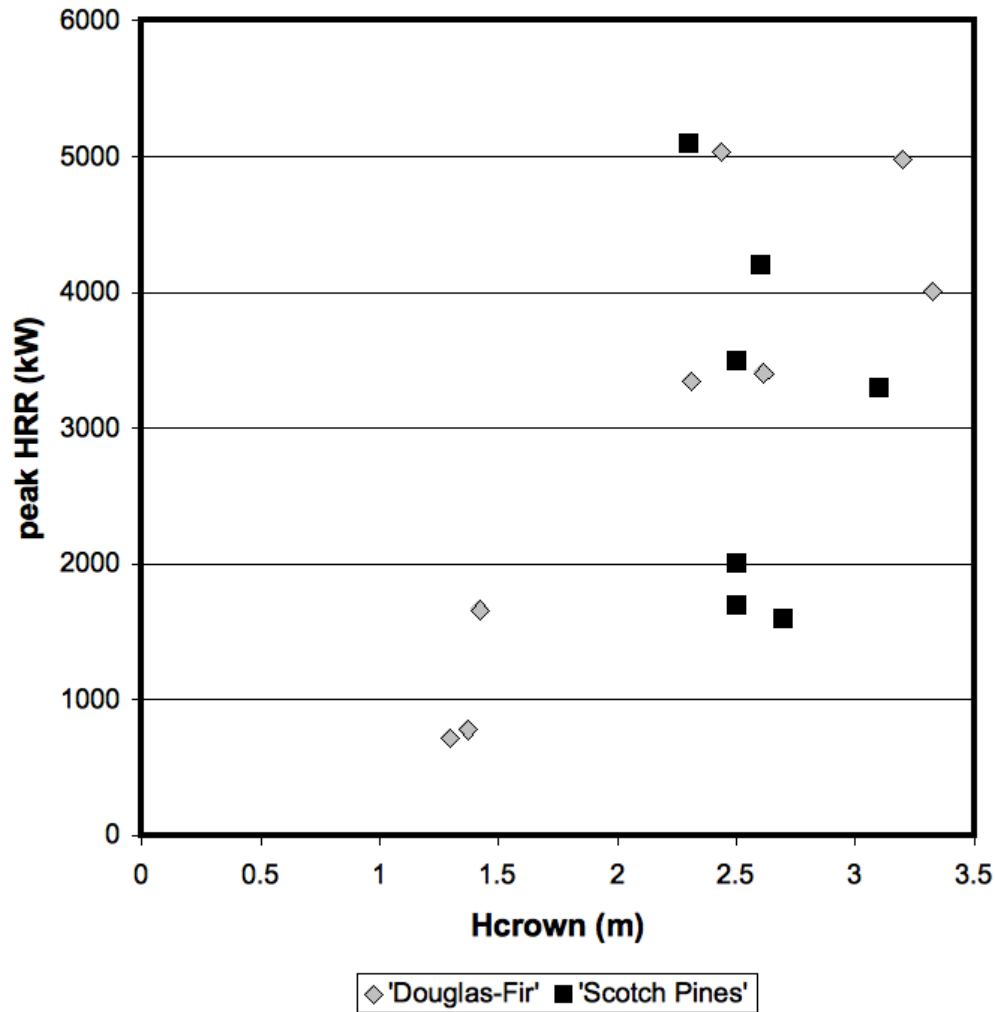


Figure 3.18: A plot showing the crown height and peak HRR for two different species of trees - the Douglas-fir trees tested in this study, and Scotch Pine trees which had been burned previously in a study on Christmas tree home ignition hazards.

As can be seen, there is considerable scatter amongst the Scotch Pines data points. The moisture content of the Scotch Pines is not known, but given that they burned to completion and were readily ignitable, it can be assumed they were in regime one (very dry trees). Likewise, the height measurements may not match

crown height used in this study. Even with these unknowns, it would appear likely that the results from this study are somewhat applicable to at least one other similar type of tree, although more tests are required to resolve the amount of scatter present in the data.

Chapter 4

Exposure to Radiant Heat Before Ignition

The effect of radiant heat transfer upon a structure or plant is dependent on two aspects – the intensity of incident heat flux, and the duration of said radiant flux. It was found during the International Crown Fire Modeling Experiment that the incident heat flux on a structure was 30 kW/m^2 from a flame front 28 m away, with a residence time of one to two minutes. Based on this, it was decided to do extended low-flux exposures to simulate a brief high-intensity one, due to the inability to safely produce 30 kW/m^2 in a lab setting. In order to simulate the effect of an encroaching wildfire, an electric radiant panel located 60 cm from the tree was used to expose the trees to approximately 2.5 kW/m^2 radiant flux for various timescales prior to igniting them via a gas burner. The durations used for the tests were 6 minute exposure, 25 minutes, and 50 minutes, as well as a control group which was not pre-heated prior to ignition. The intent was not to heat the plants to the point of ignition, as the radiant heater was not in the part of the fire lab where large-scale testing can be done, but to see what effect the radiant pre-heating had on the fire

characteristics following a piloted ignition.

4.1 Methodology

The trees were again burned in the National Institute of Standards and Technology (NIST) Large Fire Laboratory under the largest calorimeter hood. Prior to ignition, the trees were exposed to various durations of heat flux to measure the impact of radiant pre-heating. While the trees were exposed to the radiant panels, the mass loss was recorded, to determine the rate of evaporation.

4.1.1 Instrumentation

Thermocouples were placed on a thermocouple tree such that the tips are in the foliage of the trees, as shown in Figure 4.1. There were 8 in total, spaced at 30 cm above the platform level and then every 20 cm thereafter, except for the eighth, which was at 200 cm above platform level.

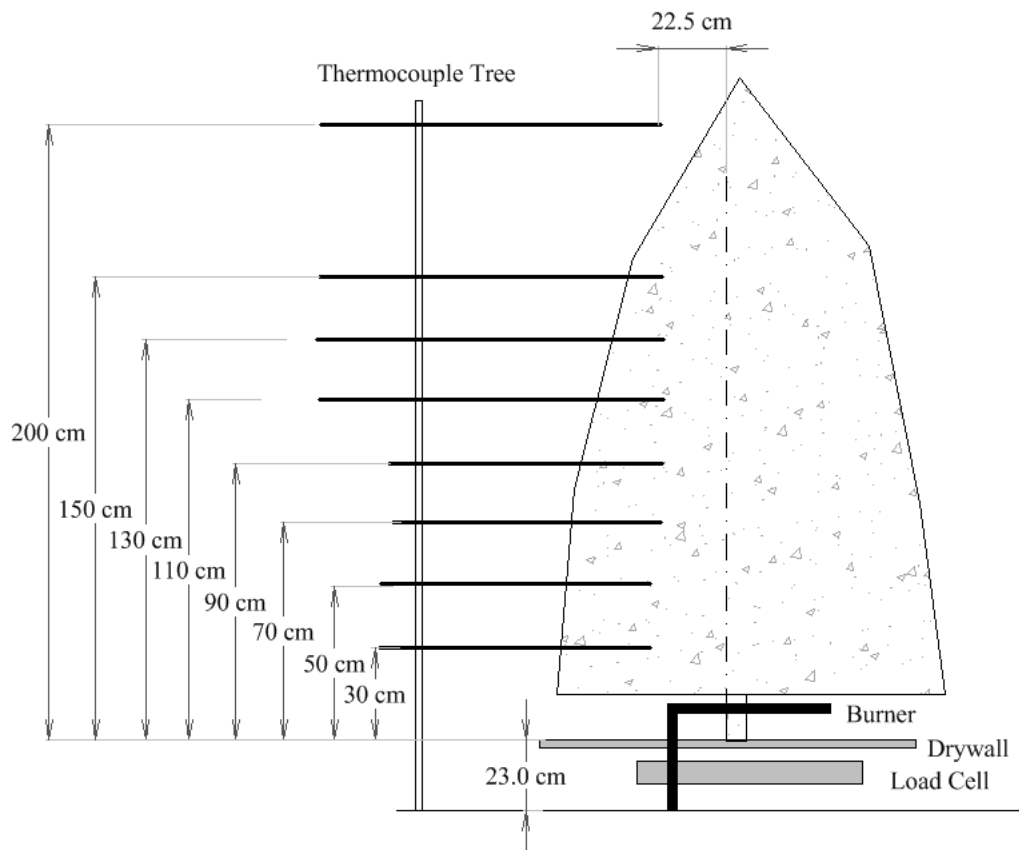


Figure 4.1: Experimental setup for the tree burns after the trees have been exposed to radiant panels showing thermocouple tree and load cell located under hood.

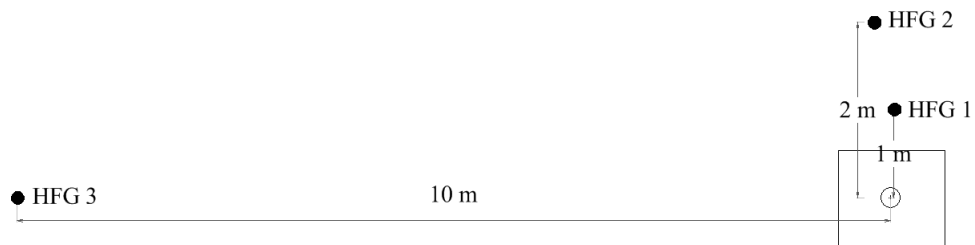


Figure 4.2: Diagram of the heat flux gauges 1 through 3 at the platform under the calorimeter hood where the trees were burned, located 1 m, 2 m and 10 m from the tree center.

Three heat flux gauges at a height of 1 m were placed near the tree when it was being burned. One was located 1 m from the center of the tree, one 2 m, and one 10 m, as shown in Figure 4.2. The gauge located 2 m from the tree was slightly offset to allow a clear line of sight to the tree without the 1-m gauge interfering. Two more gauges recorded the incident heat flux at the radiant panel while the trees were being pre-heated – one was placed near the tree’s trunk to measure the penetration through the branches, and the other was located behind the tree, as shown in Figure 4.3.

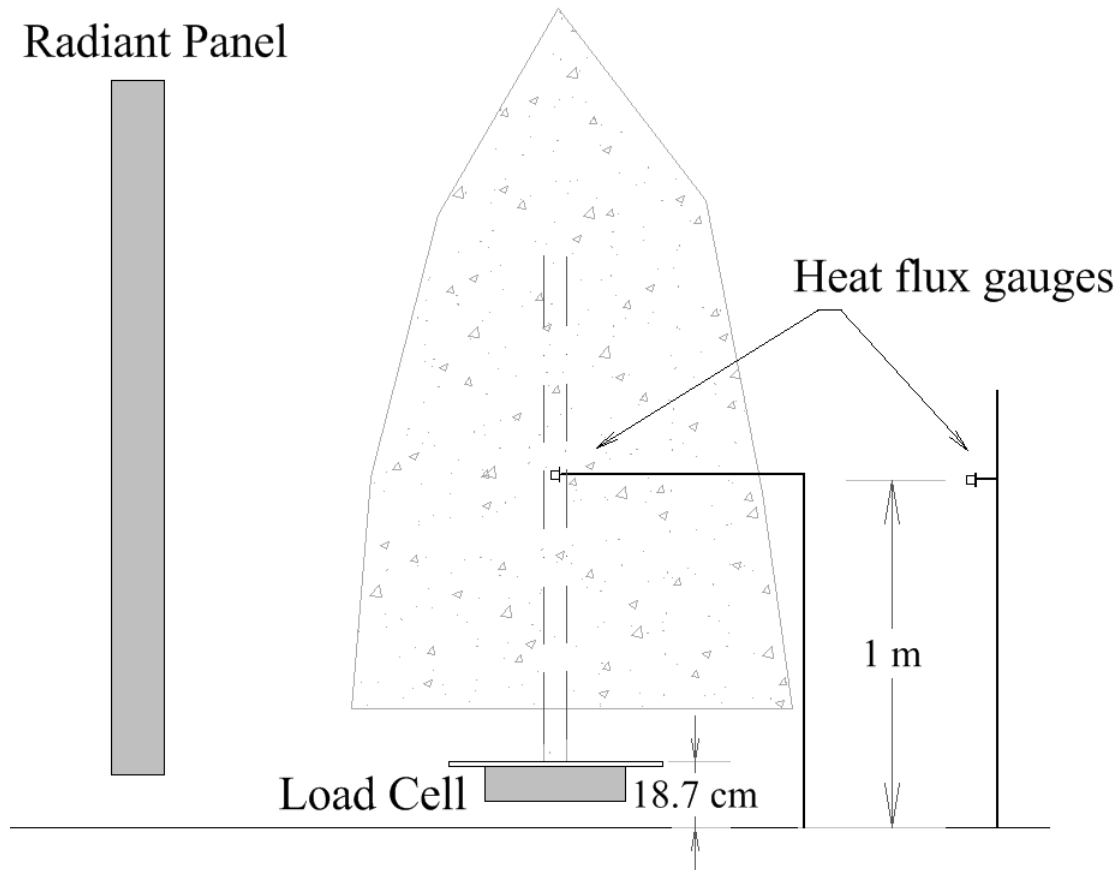


Figure 4.3: Diagram showing locations of the two heat flux gauges at the radiant panel; one in place behind the tree, and one next to the trunk of the tree.

There were a total of two load cells used in these tests. One, known as the Burn Load Cell, was located under the calorimeter hood where the trees are ignited, and used to measure mass loss rates during burning and instantaneous mass of the tree before and after exposure to the radiant panel. The second load cell, referred to as the Radiant Panel Load Cell, was located directly in front of the radiant panel. This was used to measure the mass lost as the trees were dried by the panel. The readings from the load cell were recorded by hand on a time step of 30 seconds for the duration of the radiant exposure. There is some error associated with absolute mass recorded at this load cell due to its low height, as some of the trees had branches that rested on the floor. For this reason, the Burn Load Cell was used to record the beginning mass and final mass before and after exposure for consistency and accuracy, and the Radiant Panel Load Cell was used only for mass loss purposes. The radiant panels utilized for the drying portion of the test procedure were angled inward approximately 20 degrees with a 10 cm gap between them. Each panel measures 36.4 cm wide by 198.1 cm tall, and the total distance from the left edge of the left panel to the right edge of the right panel was 83 cm. The bottom of the radiant panels was 15 cm off the floor, as shown in Figure 4.4 (a).

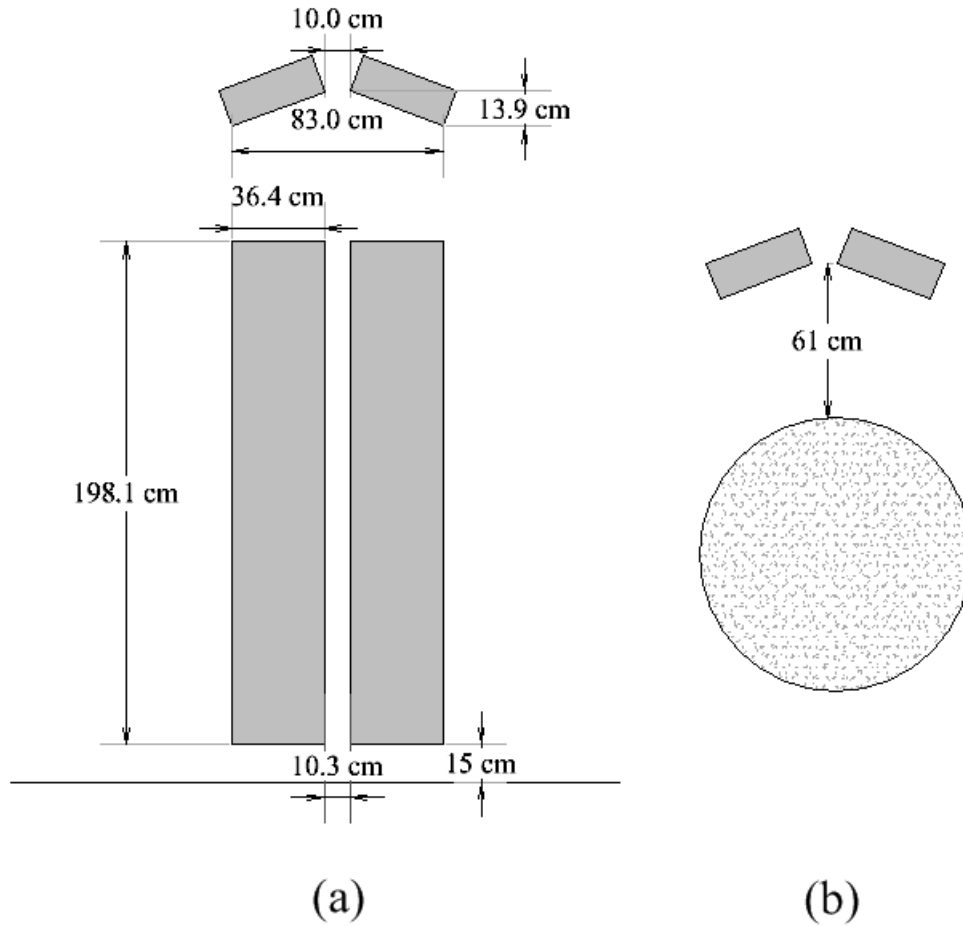


Figure 4.4: Diagram showing locations of the two heat flux gauges in place behind the tree, and next to the trunk of the tree at the radiant panel.

The radiant panel was set at approximately 430°C, and the trees were adjusted so that the widest portion was approximately 61 cm (2 ft) from the furthest point on the radiant panels (see Figure 4.4 (b)).

Before the testing began, a flux map was created at the radiant panel, to determine the incident heat flux at different locations in front of the panels, as shown in Table 4.1. At a distance of 60 cm from the panels, the incident heat flux was measured every 15 cm from the base of the panel to the top, with the gauge centered in

Table 4.1: Heat flux map created at different points in front of the radiant panels. Heat flux measurements were taken at 13 different heights along the centerline at .6 m distance and, and 3 additional measurements were taken, two 30 cm off-center, and one at .9 m distance.

Reading #	Vertical Position (m)	Distance from Panel (m)	Horizontal Position	Heat Flux (kW/m ²)
1	.30	.60	Centered	2.75
2	.45	.60	Centered	2.91
3	.60	.60	Centered	3.04
4	.75	.60	Centered	3.08
5	.90	.60	Centered	3.08
6	.105	.60	Centered	3.05
7	.120	.60	Centered	3.02
8	.135	.60	Centered	3.01
9	.150	.60	Centered	2.93
10	.165	.60	Centered	2.75
11	.180	.60	Centered	2.49
12	.195	.60	Centered	2.03
13	.75	.60	Centered	3.13
14	.75	.60	.30 m left	2.53
15	.75	.60	.30 m right	2.59
16	.165	.90	Centered	1.75

front of the panels. Additionally, two readings were taken 30 cm off-center, and one at 90 cm distance and a height of 165 cm. The largest heat flux of 3.08 kW/m² was measured at 75 cm above the bottom of the panel, as well as at 90 cm. The lowest heat flux at the top of the panel and a distance of 60 cm was 2.03 kW/m², and was 2.75 at the base. The average recorded value across all heights at the distance of 60 cm (the distance the tree was located from the panels) was 2.58 kW/m². At the height of 75 cm, and 60 cm from the panels where the largest heat flux was recorded (when centered on the panels) the values 30 cm off-center left and right averaged 2.56 kW/m².

4.1.2 Procedure

The trees were trimmed at the base of the trunk to obtain a level surface, and held upright by means of screws into a plywood stand that was 2 foot square. The stand was weighed before attachment, and its mass was subtracted from tree mass or mass loss calculations. A front face of the tree was chosen based on which side looked most uniform and didn't have a noticeable lean that would place sections too close or distant from the radiant panels, and was marked as such on the plywood stand as shown in Figure 4.5. The letters A, B, C and D were used when the trees were being photographed to indicate which face was being photographed.

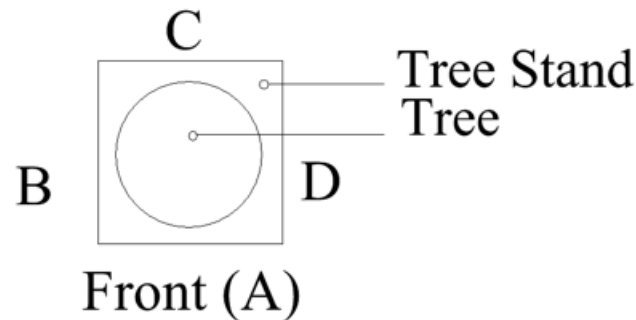


Figure 4.5: Labeling convention for tree faces used when photos were taken of all sides of the trees before the exposure to the radiant panel, and after the burn was completed.

The trees were then photographed in front of a gridded backdrop (Figure 4.6) to facilitate measuring the leaf area from digital photos. The trees were photographed from 4 directions, rotating 90 degrees each time, and the photos were labeled A through D in accordance with Figure 4.5.

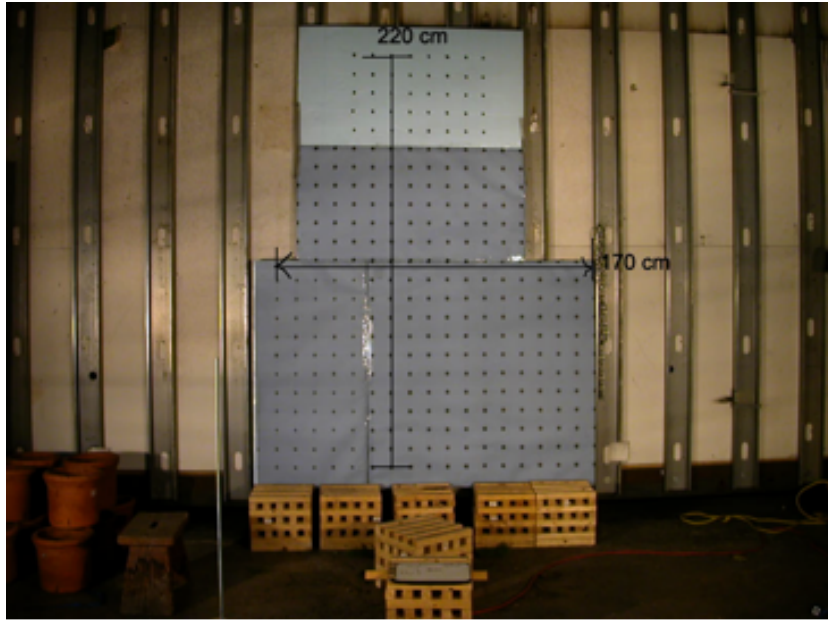


Figure 4.6: This photo shows the gridded backdrop used for photos so that the area of the trees could be later measured using a computer software program.

To obtain the moisture content prior to testing, samples of needle clusters were taken. The samples were taken from the new growth needles on the ends of the branches in 2-3 inch lengths, with each sample being comprised of three or four branch tips. Samples were taken from 3 points on the front face of each tree corresponding to the top, middle and bottom thirds, and three corresponding points on the back face as shown in Figure 4.7. A seventh sampling was taken from the front middle section consisting of older growth needles located on the middle of the branch to measure penetration into the tree from the radiant panel, and compare overall moisture differences between new and old needles. Needle samples, once collected, were either tested immediately with the moisture content analyzer, or sealed in an air-tight bag to be tested at the end of the day.



Figure 4.7: Sampling points for the needles taken to measure moisture content are shown here. Samples were taken from the bottom, middle, and top thirds of the tree, labeled as points 1, 2 and 3, from the front and rear faces of the tree.

After samples were taken for moisture content testing, the tree was placed on the Burn Load Cell and the weight recorded. Then it was moved to the Radiant Panel Load Cell and placed so that the front of the tree faced the panels. The pre-exposure mass was recorded as the starting point for the mass lost over the duration of exposure. While the mass was being recorded, the tree was shielded from the radiant panel by a section of sheetrock on a movable track. The radiant

panel was at full operational temperature for the duration of testing each day, so there was no delay from the start of the timed exposure to the desired heat flux. At the point when the timed exposure began, the sheetrock shielding the front of the panel was slid back exposing the tree.

There were two video cameras recording at the Radiant Panel, one of which recorded infrared images. A heat flux gauge located on the far side of the tree measured the permeability of the plants; or how much radiant heat flux was able to pass through the foliage.

When the timed exposure was completed, the final mass was noted and the tree was moved back to the Burn Load Cell, where the mass is recorded again, and needle samples were taken to compare the moisture contents before and after heating. The samples were taken from the same locations on the front and back face of the tree as done previously. The mass was recorded again after the sampling process was complete.

For the start of the burning section the tree was placed in the burner with the previously-established front facing towards the bottom of the U shaped methane burner. The burner consists of approximately 2 cm diameter stainless steel piping in a U shape with 46, 2 mm holes drilled every 2 cm that flows around 25 liters per minute to produce a 15-kW ignition source (see Figure 4.8). The gas piping was supported by a low platform to the side of the load cell and drywall the tree was placed on, as shown in Figure 4.9.

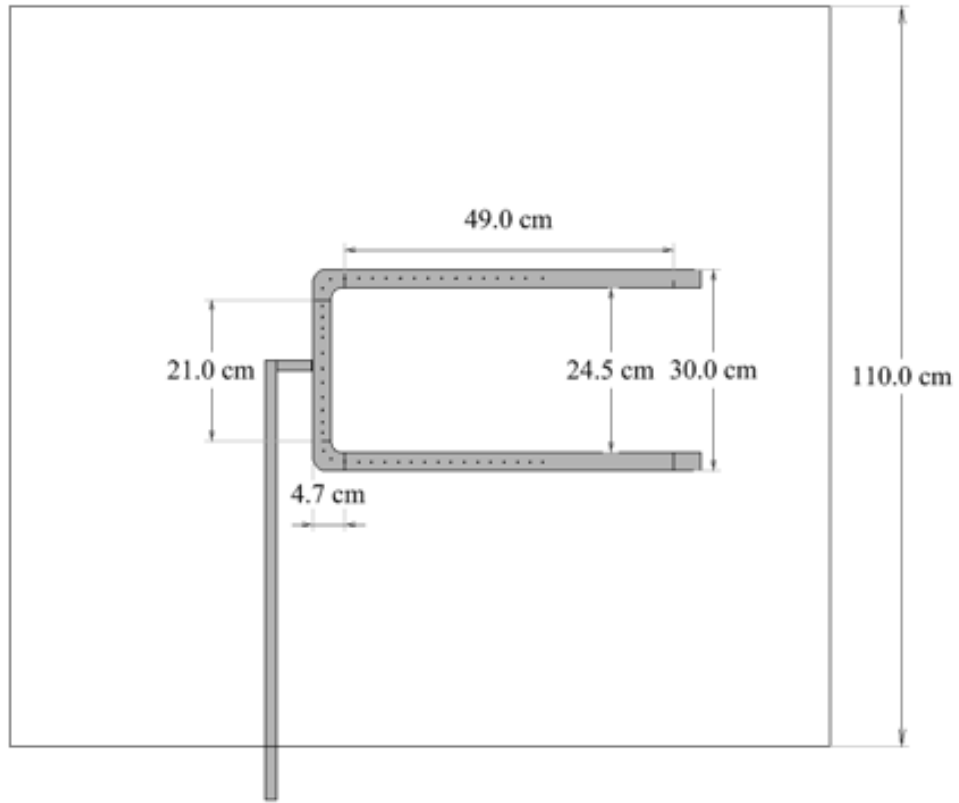


Figure 4.8: Plan view diagram of methane burner used for ignition of trees.

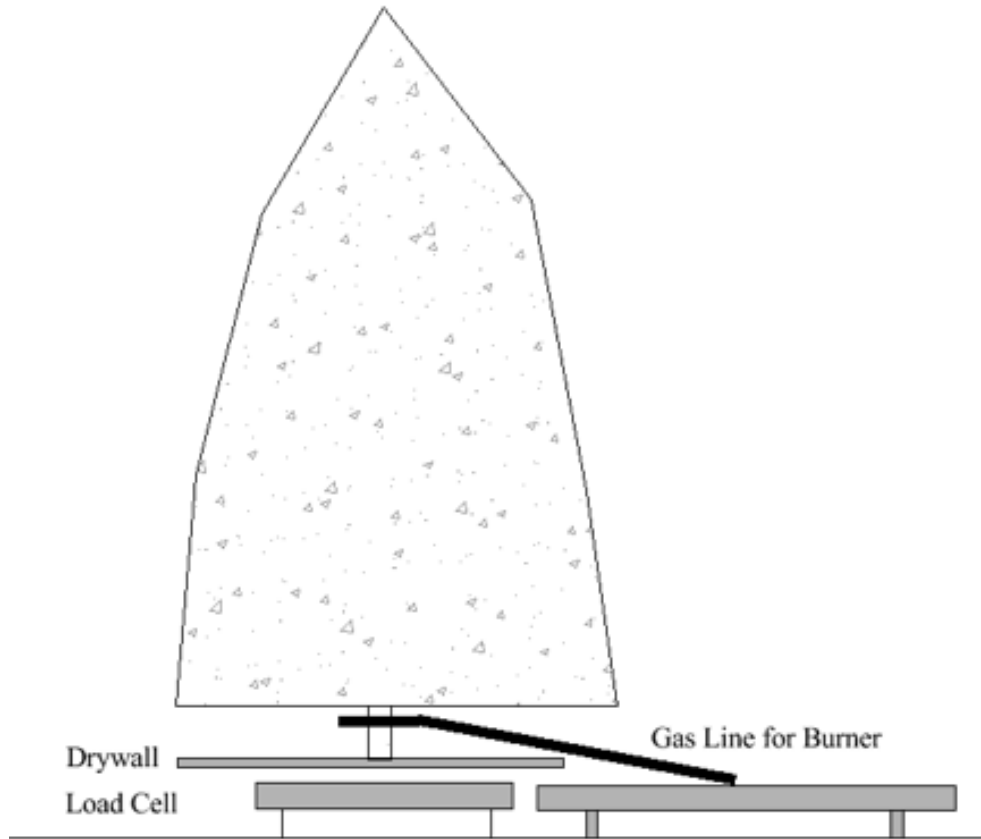


Figure 4.9: Side profile diagram of gas burner used for ignition of trees, also showing the position of the tree relative to the burner when in place for ignition.

The three cameras recording the test from different vantage points, two regular and one infrared, were activated prior to ignition. At the start of the test the valve controlling gas supply to the burner was opened, and the burner lit with a propane torch. The flames reached approximately 12 cm tall and reach the lowermost branches, simulating a grass fire that might ignite a landscaping tree, as shown in Figure 4.10. The burner remained on for 2 minutes. When the tree was completely finished burning, the final mass was recorded from the Burn Load Cell.



Figure 4.10: Photo of flames, reaching approximately 12 cm high, from the gas burner used to ignite trees.

4.2 Results and Analysis

This section will delve into the results obtained from the instrumentation in place, as well subsequent analysis performed on the data and images. For the purpose of identifying the trees, they are referred to by the exposure duration – i.e. 6-1, 6-2 and 6-3 are the three trees exposed for 6 minutes. Similarly, 25-1 was exposed for 25 minutes. C-1, C-2 and C-3 are the control trees, which were not pre-heated at all prior to ignition.

4.2.1 Moisture Content

For this group of tests, an Arizona Instruments Computrac Max2000XL moisture analyzer was used, in place of the Max1000 used earlier. The instruments share the same hardware and algorithms, the only difference being extra features and export options available with the 2000XL, which were not used. For the purpose of classifying the moisture content regime, the samples taken from the middle section of the front of the trees were used, as the trees in the first test series were sampled from that location. The differences in moisture content from the top section of the trees to the bottom was noticeable, with the top branches being lower in moisture. On average, samples taken from the top third of the trees had 93% of the moisture content from the lower samples. However, all samples taken were in excess of 130% moisture content, placing the trees well into regime 3. Figure 4.11 depicts the moisture content from samples taken from the front middle section of each tree before and after being exposed to the radiant panel for different lengths of time. Trees that experienced 6 minutes exposure did not lose a significant amount of moisture. However trees that were exposed for the longer periods of time, 25 and 50 minutes, lost between 17% to 75% of their moisture from the middle-front section with the most extreme case belonging to the third tree in the 50-minute set.

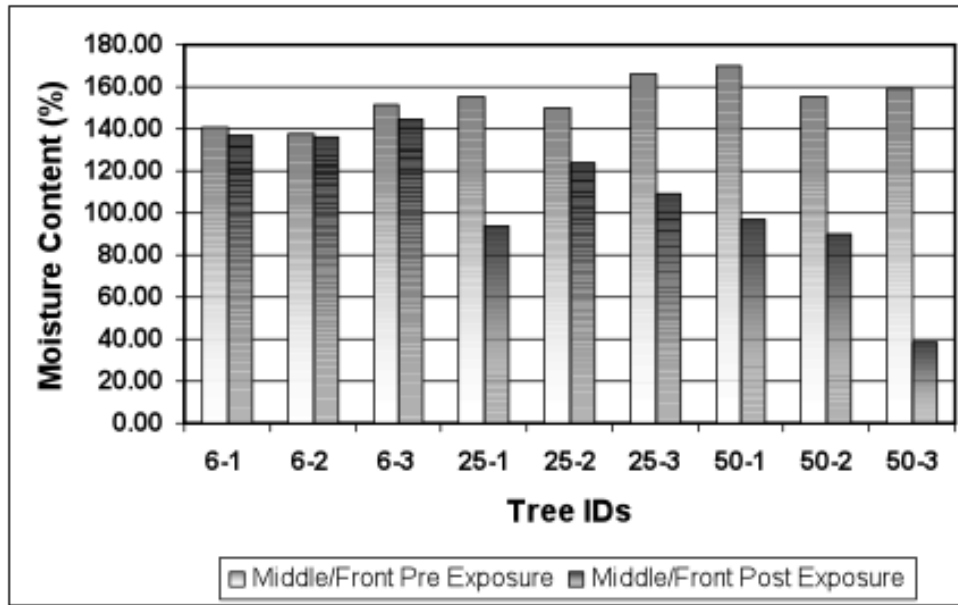


Figure 4.11: Bar graph showing the measured moisture content from samples taken from the front middle section of the trees before and after exposure to the radiant panels for differing lengths of time.

The average for the 25-minute set was a loss of 30%, whereas the average was a 50% reduction in moisture over 50 minutes. However, these reductions in moisture content only reflect the front center section of the tree, which was expected to be the most effected by the preheating. The other sections of the trees were also sampled and tested to discover how much heat would pass through the trees foliage, for instance. The moisture contents obtained from the front top and bottom samples showed similar rates of drying compared to the middle section. The back side of the tree, however, showed little to no signs of dehydration. Figure 4.12 shows the percentage drop in moisture content for all six sampling points from the 9 trees exposed to the radiant panel. The error associated with measuring the moisture content is likely around 5% due to variation among needles and twigs. Samples

taken from the back side of the tree before and after they were exposed to the radiant heat show a loss of at most 5%, and in some cases a gain in moisture content. Given the range of error, and an average across 27 samples of a 2.5% loss, it seems evident that there was no appreciable effect on the far side of the tree in terms of moisture loss due to radiant heat flux, in particular given the trees' high moisture content starting point.

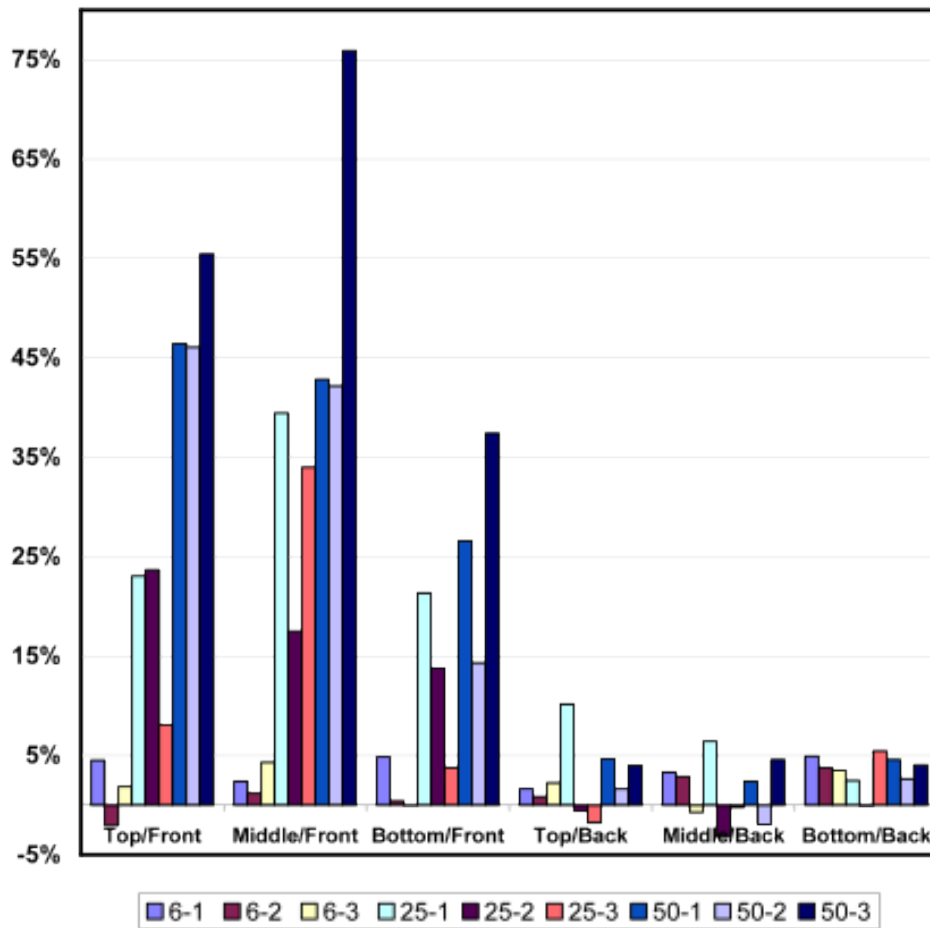


Figure 4.12: The percentage drop in moisture content for 9 trees sampled in 6 different places - three on the side facing the radiant panel, and three on the far side. Samples taken from the back side of the tree showed negligible drops in moisture content.

From the fact that only half the tree was affected by the pre-heating, it is difficult to determine exactly what the overall moisture content of each tree was at the time they were burned. Taking the average of the six sampling points will provide at least an idea, however. The average of all points sampled after the pre-heating is presented in Table 4.2, with the exception of C1, C2, and C3, which as the control

trees were not pre-heated at all.

Table 4.2: The average moisture content from six sampling points of the trees after exposure to radiant heat flux for various durations of time.

Tree ID	MC (%)
C1	151
C2	151
C3	153
6-1	141
6-2	136
6-3	148
25-1	138
25-2	140
25-3	149
50-1	134
50-2	122
50-3	110

4.2.2 Mass Loss

During the portion of the test in which the trees are exposed to radiant heat, the mass loss was recorded to determine what percentage of the water mass was lost. For the first three exposures, of 6 minutes, an average of 0.43% mass was lost. The second exposures, which lasted for 25 minutes had an average loss of 1.29%, and the final exposure of 50 minutes has an average loss of 2.75%. During the actual burning, the mass loss was also recorded. It was previously noted from the first series

of tests that the very dry trees in moisture content regime 1 and 2 lost anywhere from 27% to 67% of their starting mass. The trees in this series remained at high enough moisture content even after pre-heating that they did not fully burn, and lost an average of 6.1% of their total mass during the burn phase.

4.2.3 Heat Release Rates

The heat release rate curves for the trees burned in this phase of tests exhibited a different pattern than those discussed in the previous chapter. Due to their higher average moisture content, placing them well into regime three (as defined in section 3.2.1) which translates to a low probability of sustained burning they did not burn to completion; rather, only a small quadrant of the tree would burn and then self-extinguish. However, in six of the tests, after the first die down the tree would briefly flare up again to produce a second HRR curve, which typically had a lower peak value and shorter duration than the first one. In one instance, the second peak was larger. The second-peak phenomena was most likely as a result of the burner remaining on and progressively drying to lower branches until a second flare-up occurred. As noted by Babrauskas et al. in *Flammability of Cut Christmas Trees*, in flammability tests done with 15 cm Douglas-Fir branches, once the samples were removed from the ignition source if they were in excess of 80% moisture content, they would self-extinguish with no further flame spread. [5] For this reason, for the purpose of comparison to the first tree tests which used an ignition source that was removed as soon as the tree was burning, the second peak was discounted for analysis. This allowed the trees to be investigated using the same pattern of a single peak for the purpose of peak HRR and total heat released.

The first step to calculate the peak HRR and total heat released was to normalize the HRR plots to account for drift as the testing day continued. Drift occurs as the

moisture traps of the calorimeter become saturated and show a falsely elevated HRR as time continues. In order to account for drift, a moving average is taken 30 seconds before and after the test ends, and that number is used to set the baseline to zero kW. In addition to drift, these tests used a methane burner for ignition, so the heat contributed by the burner needs to be deducted from the total heat. The burner contribution is a known value, and that amount is deducted from the HRR. This produces data that reflect the heat contribution of the burning tree only.

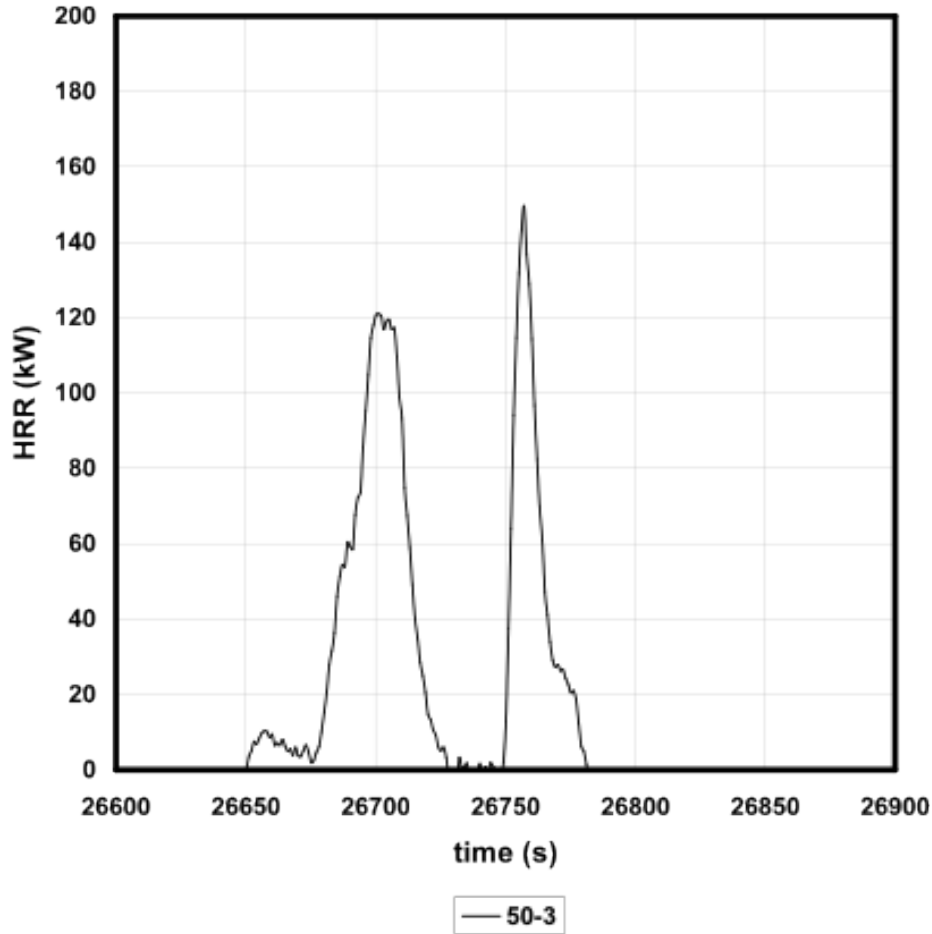


Figure 4.13: HRR-time curve for a tree that has been exposed to radiant heat for 50 minutes and then ignited, showing the dual-peak phenomenon that some of the trees exhibited.

Figure 4.13 depicts the dual-peak HRR curve mentioned above. This particular tree was exposed to approximately 2.5 kW/m^2 incident heat flux for a duration of 50 minutes prior to ignition. The individual HRR curves for the remaining 11 trees tested in this series can be seen in Appendix A. As can be seen from the graph, the peak HRR was quite low, at only 120 kW for the first peak. This is due to the high moisture content of the trees, even after a 50-minute exposure, the overall average

moisture remained high, and prevented the tree from burning to completion. The highest peak HRR measured from the trees burned in this series was 312 kW, and the average peak was 160 kW. This is comparable to the result from the first series, in which the one tree in regime 3 had a mass twice that of these trees at 38 kg, and a peak HRR of 855 kW.

4.2.4 Leaf Area

The leaf area for the trees burned in this series of tests was calculated in the same manner as discussed previously in section 3.2.4. Digital photographs of the trees were taken before testing, with the addition of a gridded backdrop to aid in scaling the tree's height. This is a method less prone to user error, as the original method relied on having an accurate measurement of the crown height, and being able to relate that measurement to the photo at hand. The crown height was measured from the bottom-most branch to the base of the upper shoot, but those points were at times difficult to establish from the photo. By using the grid to scale the measured areas, a consistent pixel to actual length relationship was used in each measurement. Figure 4.14 shows an example tree in front of the backdrop. When the photo was calibrated, the software program would measure the distance in pixels between two user-specified points, A and B in this photo, and the actual value in meters was entered. This produces accurate measurements of the tree's leaf area in square meters.



Figure 4.14: Photo a one of the trees prior to being burned in front of the grid backdrop used to calibrate distances in the digital photos for the purpose of measuring the leaf area, where the distance between 'A' and 'B' is known.

Each tree was measured from two different photographs taken at 90° rotations to account for any uneven growth in one direction. These trees, unlike those burned in the first series of tests, were very similar in height and diameter, and had very similar leaf areas. The results from this test were plotted against tree mass in conjunction with the same results obtained from the first trees burned, to further

test the validity of the tree mass to leaf area relationship.

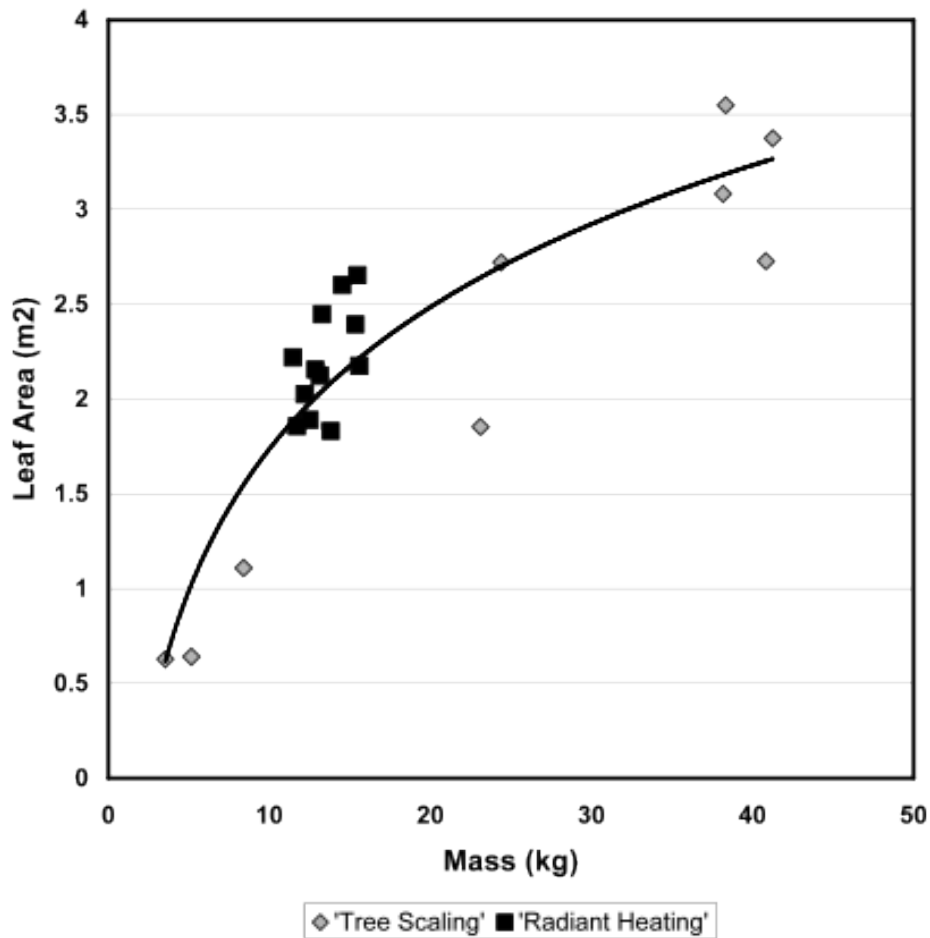


Figure 4.15: Chart showing the relationship between leaf area and tree mass for trees from both the first and second series of tests, which were obtained from different tree farms.

It can be seen in Figure 4.15 that the data points from this series of tests, denoted as 'Radiant Heating,' fall in roughly the appropriate area as compared to data points from the previous section. However, as an example, for a tree with a leaf area of 1.8 m² the corresponding mass within the scatter of data could relate to a tree of 11 kg, or one of almost 25 kg. The problem lies with the different sizes or thicknesses of

trunk, which can vary depending on a trees age, health, and also at what height the tree was cut. However, as the trunk and large branches barely contribute to the fire size, it is not ideal to base fire size predictions off of something so arbitrary. In the future, one possibility would be to develop a relationship that eliminated the need for mass altogether, and instead use leaf area to directly predict HRR and other characteristics in conjunction with the moisture content.

Chapter 5

Fire Spread Amongst Closely Grouped Trees

The purpose of this series of tests was to determine how readily fire would spread from one burning tree to a nearby tree, with the variables being tree spacing and moisture content. All the trees used in this series were the same approximate age, height and mass. They were obtained from the same tree farm and were cut on the same day, July 31 2003. The trees were divided into either dry or wet categories. The former were allowed to air dry inside the large fire lab for the 3 weeks between when they were cut and testing began on August 21, and the latter were kept well-watered to keep their moisture content higher. It was found that amongst the watered trees, some trees retained more moisture than others, as indicated by needle loss and discoloration. Based on visual observations prior to testing, the trees were categorized as very dry, moderately dry, or wet.

From needle samples taken at the time, frozen, and later tested (at the same time as the samples taken from the first tests) the very dry trees has a needle moisture content of around 15% and the wet trees were around 60%. Based on the moisture

content, they can be placed in regime one and two of the moisture content band as established previously. However, not every tree was sampled, and therefore the moisture contents must be taken only as an indication of the approximate level of moisture, not an absolute. The setup for the tests followed a slightly different procedure than the tests described in previous sections. Rather than burning individual trees, for this phase of testing groups of trees, between two and four at a time, were burned together. The trees were placed in a line on a diagonal across the platform, and the spacing between them was changed from test to test but varied from 3 in to 12 in. The spacing was measured from the widest part of the tree, typically at about one third of the crown height measured from the base of the tree. The trees were arranged on a large platform which was supported by 4 load cells, the readings of which were totaled. This platform was located underneath the large hood for calorimetry measurements. One heat flux gauge was placed 1.8 m (6 ft) perpendicular to the centerline the trees were lined up along, as illustrated in Figure 5.1.

5.1 Procedure

The first test consisted of four dry trees, ID numbers 1, 7, 10, and 13, spaced 1 foot apart in a line. One tree, known as the ignition tree (as denoted in Figure 5.1), was ignited by means of a propane torch that was held for 3 seconds on the left side of the trunk at the lower branches, and then 3 seconds on the right side. Although tree #7 burned vigorously, the fire did not spread to the adjacent tree (#10). Tree #7 was discarded and the remaining trees were then shifted so that they were only 6 in apart, and tree #10 became the ignition tree. Using the same procedure, tree #10 was ignited, and again the fire did not spread to the neighboring trees. At that

point, tree #13 was ignited with the torch, while still 6 in from tree #1, with the same result, there was no fire spread. However tree #1 was singed somewhat on the outermost needles on the side that was closest to tree #13.

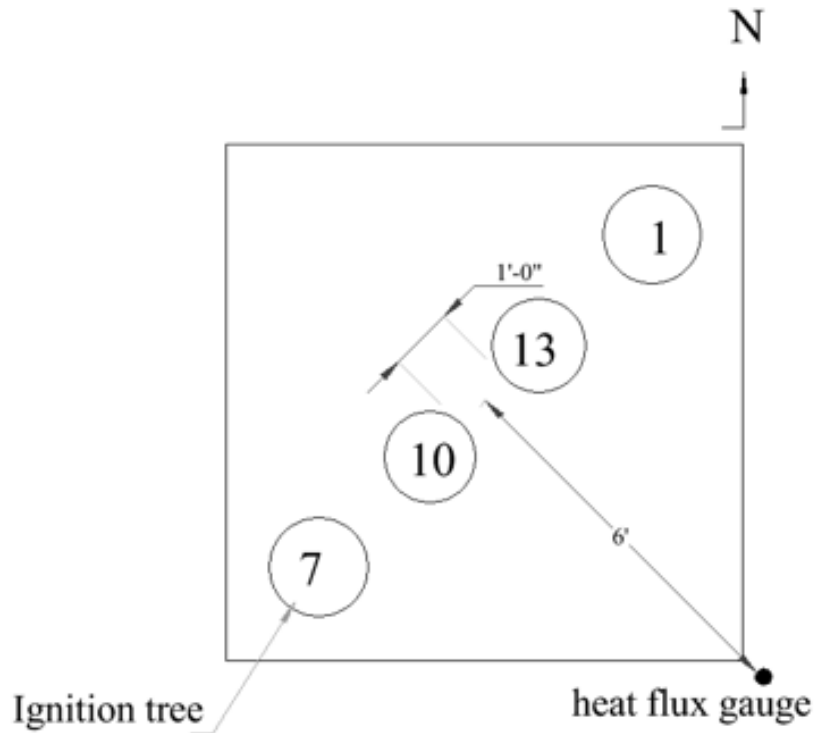


Figure 5.1: Experimental setup for fire spread experiments test 1; 4 trees spaced at 1 foot apart

The second test took the unburned tree from test 1, tree #1 which was singed but not ignited, and placed it next to a new tree (#9) which was also from the dry group at a distance of 3 in as shown in Figure 5.2. Tree #1 was ignited and although tree #9 started smoking after 30 seconds, it still did not ignite before tree #1 self-extinguished.

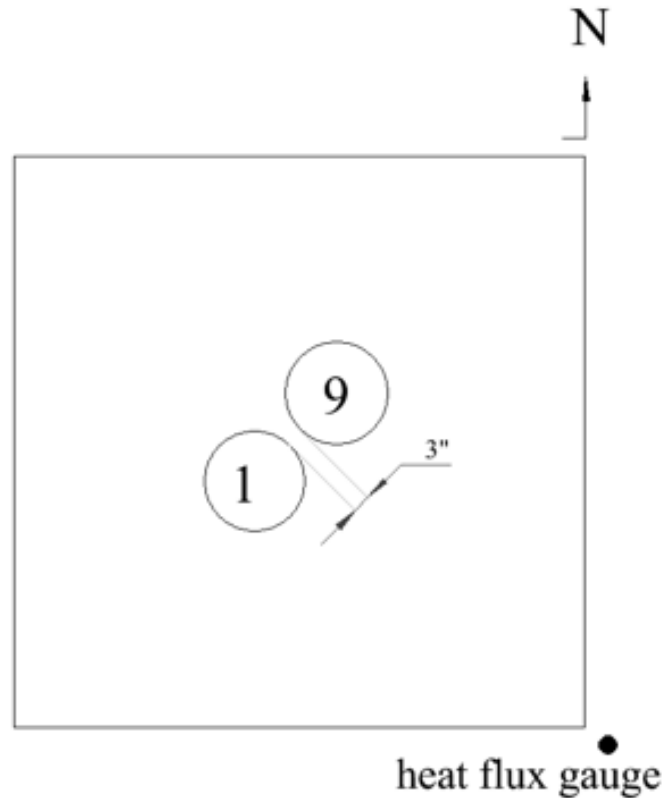


Figure 5.2: Experimental setup for fire spread experiments test 2; two trees spaced at 3 in

Test 3 involved four new trees, these ones from the moderately dry moisture content group, set up the same way in a straight line with 0.152 m (6 in) spacing between trees. Based on the results from the first two tests with no fire spread using dryer trees, it could be assumed that the fire would not spread in quiescent conditions, therefore these tests had the addition of a large fan located 3.15 m (124 in) away aimed at the ignition tree to facilitate fire spread, as illustrated in Figure ???. The presence of wind produced a deflection of the fire plume. This deflection led to ignition of neighboring trees due to either impingement of flames or increased levels of radiant heat flux due to the flames' proximity.

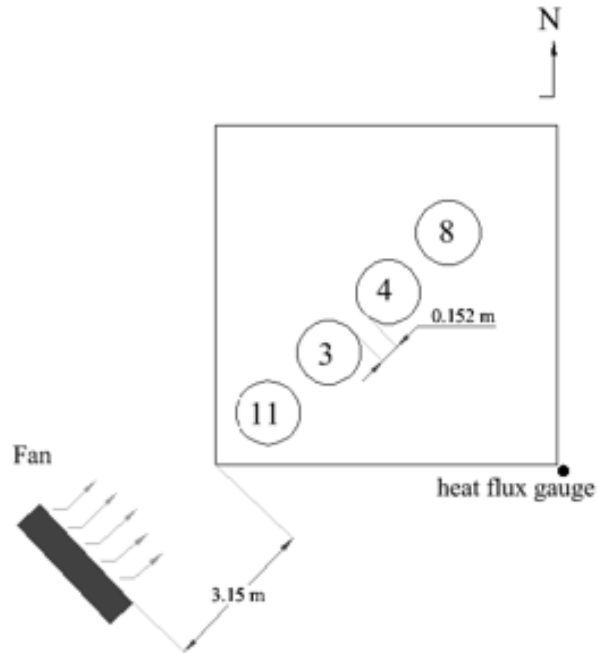


Figure 5.3: Experimental setup for fire spread experiments test 3; tree spacing at 6 in with inclusion of fan at 3.15 m – diagram not to scale.

Tree #11 was ignited in the same manner as before, with a 3 second application of the torch to the left side, and a three second application on the right. At the 6 second mark, the fan was turned on. However, the wind velocity was high enough as to prevent the fire from becoming well-established. The end result was that the ignition tree did not burn at all on the side closest to the fan, and only weakly on the leeward side. However, the fire plume did impinge on tree #3 which ignited. Tree #3, once ignited, burned for 25 seconds with a fire plume which never grew taller than 0.9 meters due to the wind affect. The fire did not spread beyond tree #3. Test 4 took the unaffected trees, #8 and #4, and added one more, #12 which was also moderately dry. For this test, the fan was moved farther away, to a distance of 7.42 m (292 in). The trees remained at 0.152 m spacing as shown in Figure 5.4.

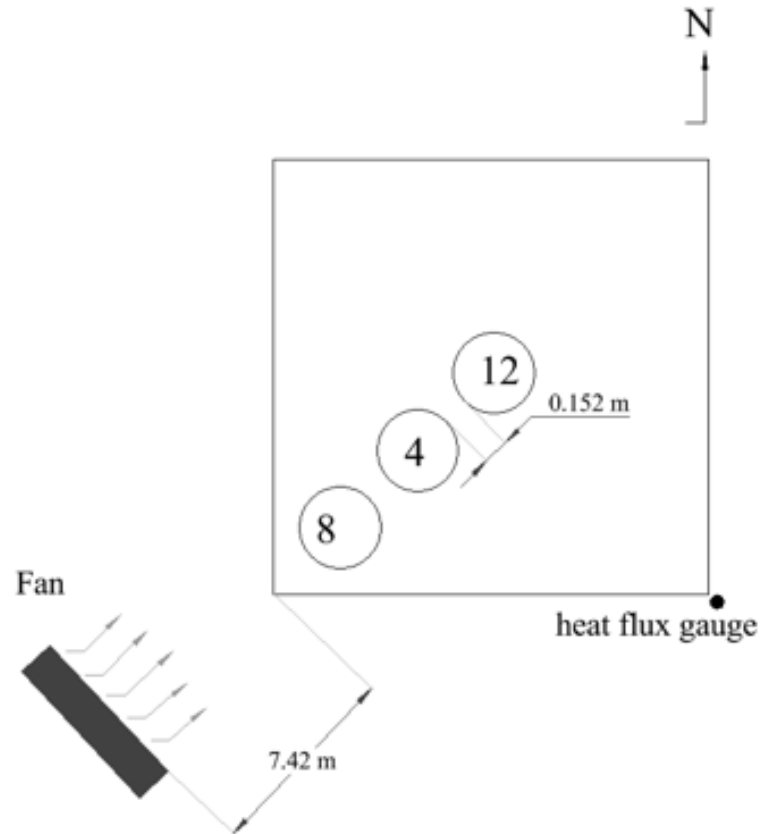


Figure 5.4: Experimental setup for fire spread experiments test 4; tree spacing at 6 in, fan at 7.42 m

Locating the fan at a greater distance resulted in fire spread from tree #8 to #4 and the brief ignition of tree #12. The wind speed velocity was not measured at the time; however, by using the flame angle taken from a video capture, the approximate velocity can be deduced. Figure 5.5 shows a video capture taken of test number four from the east camera. The angle between the tree bases and the flame is 69° . The east camera was not exactly perpendicular to the trees, so this angle measurement is likely somewhat skewed. For the purpose of estimating wind velocity, an angle of 70° was used.



Figure 5.5: Video capture from test 4 showing the flame angle due to wind as flames spread from tree #4 to tree #12.

G. Heskestad has compiled a chart depicting flame deflection angles for flames in wind, plotted against a ratio of u_w/u_{oL} which is the wind speed over the mean axial velocity at the flame tip. [13] The data differentiates amongst different L/D ratios, or flame height to diameter; however, the difference is negligible amongst the scatter and was not considered here. In order to calculate the axial velocity at the flame tip, the following equation was used, which calculated the maximum upward velocity in a fire plume at the intermittent flame (or flame tip).

$$u_o(max) = 1.9Q_c^{1/5}m/s \quad (5.1)$$

In the case of test 4, the peak HRR was approximately 1000kW, so the maximum axial velocity would be 7.5 m/s from the above equation. Using the flame deflection chart mentioned previously, the wind speed for a deflection of 70° (or 20° from the vertical, as the chart is arranged) and plume velocity of 7.5 m/s, the wind velocity would be in the range of 0.5 m/s to 0.8 m/s. A rule of thumb mentioned in *Introduction to Fire Dynamics* is that a wind speed of 2 m/s will deflect a flame by around 45°. [13]

Test 5 repeated the setup from test 4, with 6 in spacing, but using three trees from the "wet" group, trees #6, #2 and #5 as shown in 5.6 The fan was kept same distance (7.42 m). Tree #6 was very resistant to ignition, and even with the torch held in place for 15 seconds, it didn't sustain burning for more than 20 seconds, with very small flames. The fire spread through the center portion of the tree, which had a greater proportion of dead or very dry needles; none of the outer branches burned. As such, the fire did not spread beyond the ignition tree.

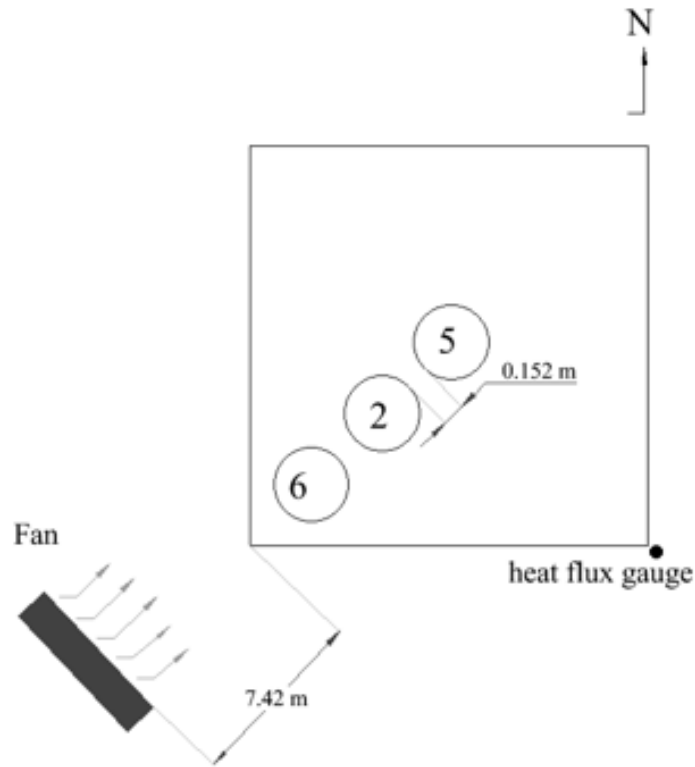


Figure 5.6: Experimental setup for fire spread experiments test 5; tree spacing at 6 in, fan at 7.42 m

For the final test, trees 2 and 5 were used again along with tree #15. This test was to determine if the trees would ignite when exposed to radiant heating from a 2 MW heptane burner fire in a quiescent atmosphere. The trees were spaced so that they were located 40.5 in, 64 in, and 85 in from the burner, measured to the tip of the tree. The burner was located 4 ft above the tree bases. The layout and dimensions of the experimental setup are shown in Figure 5.7.

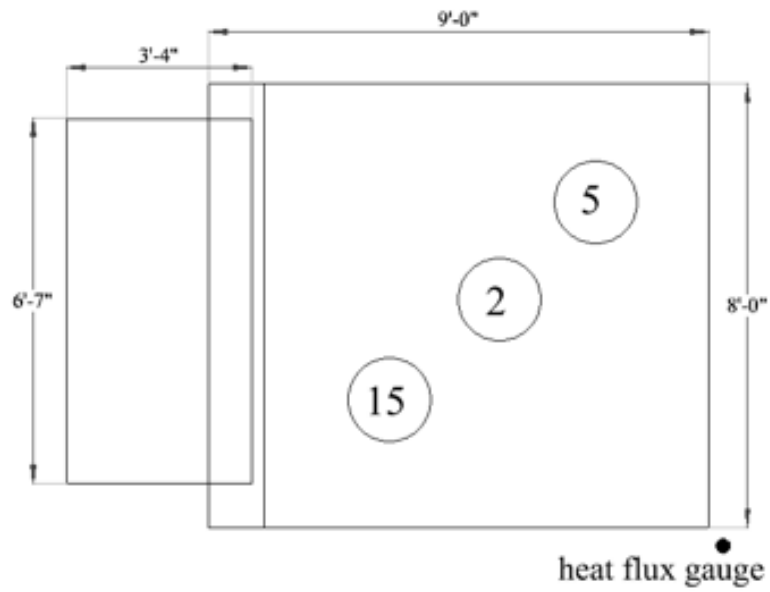


Figure 5.7: Experimental setup for fire spread experiments test 6 with a 2 MW heptane burner located next to 3 trees of high moisture content.



Figure 5.8: Photo of heptane burner heating a cluster of trees as part of fire spread experiments.

The burner was ignited and the trees were observed for signs of smoke, needles growing brown, or flame. At 17 minutes, the tips of the trees were smoking very lightly, as can be seen in Figure 5.8. At that point, trees #15 and #2 were ignited via the same propane lighter as used previously. Both trees ignited, however only the center portions burned, for the most part the outermost portions of the tree were resistant to burning. Tree #5, which was not directly ignited by a torch showed signs of singed needles, but did not ignite.

5.2 Results and Analysis

The impact of moisture content on heat release rates has been established in the previous chapter, so it was not analyzed as fully here. The first four trees burned, encompassed in tests 1 and 2 of this series, were all very dry trees approximately in regime one of moisture content. All four trees, in the absence of any wind movement, burned independently with no fire spread, and can be treated as individual tree fires. The relationship between the tree mass and its peak HRR was compared to the same data for the 4-foot trees burned in the first series of tests as described in Chapter 3. The trees burned in the two test series were the same species, however they were obtained a year apart from different tree farms. It can be seen in Figure 5.9 that the two test series have a large degree of scatter, but a trend is apparent. One reason that may account for the disparity is that at the lower range of mass for this species of trees, small trees around 2 kg, the majority of that mass is naturally the trunk. The trees from the first series of tests had a comparatively low leaf area versus the trees burned in the final series. Precise leaf areas are not available for the fire spread tests trees, but they were visually much fuller and more densely needled, which could account for the somewhat higher heat release rates.

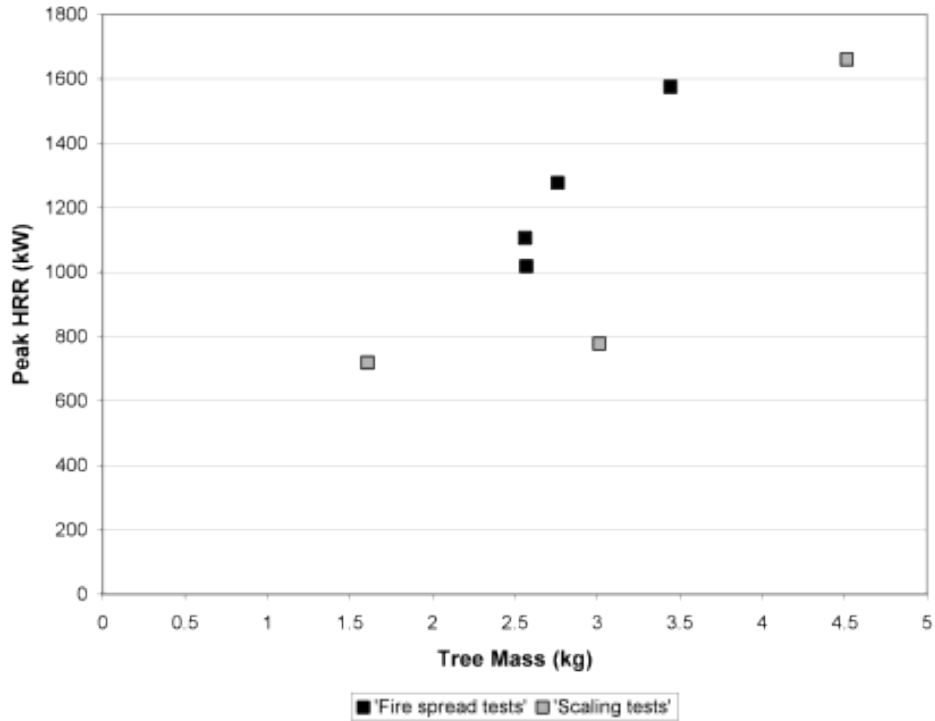


Figure 5.9: Comparison of mass and peak HRR for the 4-foot trees burned in the first series, tree variation and scaling, and last series of tests, flame spread.

Table 5.1 shows the peak HRRs recorded for each test in this series. Test one was actually composed of three individual tree burns for all intents and purposes; those are labeled 1a, 1b and 1c. What this table illustrates is the significant decrease in peak HRR for the wet trees, even in the presence of wind. In the case of tests three and four, even though two trees were burning instead of one, the peak HRR was still lower than the very dry trees burning individually.

Table 5.1: The peak HRRs for the trees burned as part of the test series on fire spread.

Tree IDs Involved in Test	Test	Peak HRR (kw)
7	1a	1106
10	1b	1277
13	1c	1575
9, 1	2	1018
11, 3	3	905
8, 4, 12	4	993
6, 2, 5	5	-

Test five, which was composed of very wet trees, had such a low HRR that it did not register on the laboratory equipment. The peak HRR from test six is not included in the table because the presence of the heptane burner produced a fire signature an order of magnitude greater than that of the burning trees, making it difficult to isolate the smaller HRR. However, based on visual observations, even with preheating from the burner for 17 minutes, the trees did not fully ignite and would have had very low HRRs.

Chapter 6

Uncertainty

In order to properly evaluate the results of the full-scale fire tests and derive conclusions based on measured values, the uncertainty of those measurements needs to be known. Uncertainty can mean many things, but in this case it will refer to measurement uncertainty, or the level of confidence in the numbers reported here. Measurement uncertainty can be caused by several factors: human errors in reading a scale, imperfections in instrumentation that leads to 'systematic' errors, or random errors. Additionally, in some cases (for instance HRR) the reported value is not a direct measurement, but rather a calculated value using several measured values as input, each of which will have its own associated uncertainty – therefore there will be some propagation of the uncertainties.

The uncertainty represents the range of probable values around the measured value within which the actual value being measured most probably lies. A Type A uncertainty analysis is done with standard statistical methods. A Type B uncertainty analysis is a technique to quantify measurement uncertainty that relies on scientific judgment and available information including manufacturer's calibration reports, equipment specifications, and previous measurements.

6.1 Thermocouples

Thermocouples are constructed by joining two dissimilar metal wires to form a junction. The different metals have different rates of heat absorption, and the different temperature created a voltage potential across the junction. Type K thermocouples, for example, are a common thermocouple composed of Chromel and Alumel alloys. That voltage can be translated to a temperature when compared to the ambient temperature at the open ends. The uncertainties that arise with thermocouple temperature measurements are due to several things including differences between the temperature of the junction, and the actual gas temperature the junction is located in, and time response of the thermocouples which is a function of thermocouple material and diameter. Temperature differences are due to radiative heating or cooling of the junction, catalytic heating of the junction due to radical recombination reactions at the surface, and aerodynamic heating at high velocities. [21] For fires burning in woody fuels, however, the catalytic reactions are generally negligible for type K thermocouples. [2] The thermocouples used in these experiments were 3-mm-diameter sheathed type K thermocouples, 0.91 m (3 ft) long, with an exposed bead (non aspirated).

6.2 Heat Flux Gauges

The heat flux gauges used in these experiments were total heat flux gauges. The impact of this is that the gauge is sensitive to each mode of heat transfer (radiation, convection, and conduction) which can impact the reading that we are most interested in – that of incident radiative flux. Incident radiative heat flux cannot be measured directly, therefore there is some propagation of uncertainty through the indirect measurements required.

6.3 Heat Release Rate

In the case of heat release rate the measurement uncertainty can vary depending on the relationship between the size of the fire to the capacity of the hood. Heat release rate isn't a direct measurement, but rather is the product of a series of calculations based on measurements taken from gas samples. This can lead to a propagation of uncertainties in which each instrument has its own associated uncertainty, which must each be accounted for when assessing the final product. Additionally, uncertainty is added from the exhaust system itself due to the need for mixing and turbulence at the gas sampling point and the possibility of gas leaks that would cause underestimation of the actual HRR. For the full details of the accuracy of the individual instruments that comprise the exhaust hoods, refer to the NIST IR6509, Large Fire Research Facility (Building 205) Exhaust Hood Heat Release Rate measurement System [25].

While the 15MW exhaust hood in the Large Fire Research Facility at NIST has not been fully characterized, there is data regarding the uncertainty associated with the three smaller hoods based on a series of calibration experiments. The largest of the hoods that was characterized in the NIST IR measures 4m by 5m and has a peak HRR capacity of approximately 3MW. Using gas burners with a measured volume flow rate and natural gas that was analyzed for the breakdown of its component gases a known theoretical HRR can be calculated from the heats of combustion. This value does have its own uncertainty. The known theoretical value at different burn rates was then compared with the measured HRR from the hood. For the 3MW hood, the maximum difference between the theoretical and measured HRR was 20%. In the cases of the smaller hoods, the disparity between the two values increased as the fire size approached the maximum capacity of the hood. A

reasonable assumption for the experiments documented in this paper is that with a peak recorded HRR that is only one third of the capacity of the hood the error wouldn't be extraordinarily large, and an uncertainty of 20% as documented for the 3MW hood is a reasonable ballpark.

Chapter 7

Conclusions

Owing to the differences in burning patterns amongst the various test series, it is difficult to draw overarching conclusions. Rather, each series is considered on its own merit and the conclusions may provide guidance for future research and for fire modeling.

From the results of the experiments and analysis presented, it is clear that some scaling relationships of the burning characteristics of a Douglas-fir exist and are based on tree size and moisture content. Moisture content can be obtained fairly easily, by taking samples of tree foliage and small stems and dehydrating them. The moisture content information can be used to group trees of different hazard levels. Trees with moisture content below 30% pose an extreme hazard, as they will ignite readily and burn fully and intensely even if the ignition source is removed. Trees with moisture contents between 30% and 70% will require a larger ignition source, but will still burn to completion. Moisture contents greater than 70% the normal range for a tree that is not suffering from water deprivation result in trees that are highly resistant to ignition from anything but the most robust heat source.

Along with information on the moisture content, an estimate of the tree's mass is

needed. This can be calculated by means of height or leaf area if it is not reasonable to directly weigh the tree (i.e. it is still in-ground). The leaf area of a tree is a term that refers to the two-dimensional area of a tree that is covered with leaves or needles, and can characterize trees more precisely than height alone. An example of this situation would be when considering deciduous trees, which may have heights three times that of a conifer, but the same volume of consumable fuel in the form of leaves and small branches. The leaf area can be measured from digital photographs, and by using image analysis software it is possible to accurately measure the area of irregular-shaped tree crowns. This leads to a better indication of actual burnable mass, as in the case of individual tree fires, the trunk and large branches do not burn, but merely char.

If both the moisture content and mass of a tree can be estimate or measured, the peak HRR for a given tree size can be predicted using a curve-fit relationship of available data. With this peak HRR value, a triangular approximation of the HRR curve using a 60 second duration has been demonstrated to predict the measured total heat released with an average of 11% accuracy in the case of Douglas-fir trees. This prediction can be used to calculate the impact a particular tree may have on a nearby structure in the event of a wildland/urban interface fire, even if that particular size tree has no experimental data.

In addition to peak HRR, it is also possible to scale the flame height based on the tree size. This can be used for calculating radiative heat flux when coupled with a flame temperature. The flame heights, as measured from the seat of burning were found to be 3 times the crown height for trees between 1 and 1.5 meters tall, and the 3-meter-tall trees had flame heights that were 1.5 times the crown height, with the 2.5-meter-tall trees falling in the middle with fire plumes 2 times their own height. A linear relationship was found relating the ratio of the crown height to the flame

height, which would allow flame height predictions based on the measurable crown height.

When the trees are exposed to radiant heat prior to testing, there was no noticeable effect at the laboratory scale on the time to ignition, peak HRR, or radiant heat flux. This was due in most part to the very high moisture content of the trees to start with – well into regime 3. Even when exposed to 2.5 kW/m^2 heat flux for 50 minutes, although the needles on the side closest to the radiant panel were affected, the overall moisture content of the tree remained high enough for it to resist ignition, and the trees self-extinguished upon removal of the ignition source. In addition, it was found that the low-level radiant heat flux was not able to penetrate the entire width of the trees to have an effect on the needles on the far side. It is not known how a short duration of higher heat flux would impact the penetration through the tree.

From the fire spread tests, it was shown that in the absence of wind even extremely low moisture content trees will not ignite from a neighboring tree that is burning, even if they are in close proximity to each other. However, very rarely will a wildfire occur under these conditions – due to the convective heating of the air ahead of and above a fire they will create their own wind, which can drive a fire forward, as well as producing high levels of radiant heat flux, drying the vegetation ahead of them. It was found that in the presence of wind, fire spread amongst even very wet trees was possible. However the HRRs were greatly reduced compared to the tests done with very dry trees even when two trees were burning simultaneously, and the trees quickly self-extinguished. This only emphasizes the importance of maintaining well-watered vegetation around homes in the WUI. Even in the event of a wildfire igniting landscaping trees, if they are wet enough they will resist fire spread, and self-extinguish with a minimum of damage if the ignition source is removed.

Chapter 8

Future Work

There is much to be done to understand the burning characteristics of individual trees, including validation of lab results in the field. Trees in these tests were harvested from a tree farm to control the impact of variables such as rainfall and overall health; it was assumed that they were representative of Douglas-firs. Farm-grown trees, however, may have been shaped at some point to ensure full, evenly rounded trees at Christmastime. This trimming may result in higher needle density than non-farmed trees. Reduced light penetration to interior branches is another direct consequence of shaping and may lead to an increased volume of dead needles closer to the trunk, which may, in turn, result in increased HRRs over naturally growing trees. [8] For this reason, trees that are not maintained with an eye for a pleasing shape may exhibit different results, which bears investigation.

Additionally, the differences across species of trees were wholly unexplored in this study, except for a comparison to previous data from Scotch Pine trees. However, as those trees were burned under different conditions, it cannot be considered a definitive comparison. Outside the realm of evergreen trees, deciduous trees will almost surely exhibit different burning characteristics, because volume/ surface area

ratio differences of leaves versus needles, the way the trees store water, and even the height of the understory leaves above ground level will all affect how they ignite and burn.

An ideal starting point for measuring the characteristics of individual trees may be to establish a relationship between leaf area (and to take it one step further, the *volume* of the crown) and burnable mass for a tree, and how that translates to a HRR curve. This could be done by photographing a tree to measure the leaf area, and then deconstructive sampling to obtain the mass of the leave and small branches likely to be consumed in a fire. Once the mass can be estimated in this fashion, a tree crown could be burned to obtain the HRR. The current method for predicting peak HRR is a function of moisture content and mass, which is not ideal due to the fact that the trunk comprises a large portion of the mass, but does not contribute to the HRR. Developing a relationship with leaf area substituted for mass, in conjunction with moisture content, would allow for more accurate estimations. With data such as has been obtained in this study, as well as future work, it may be possible to refine the existing fire models to the point where they can provide very accurate hazard analysis for homeowners to judge what level of risk they are at, as well as aid policy makers in forming guidelines on community firesafety.

8.1 Flux Time Product

The flux-time product, or FTP, may be more accurately understood as the flux-time integral. The FTP is simply the area under a heat flux curve, and is used as a means of quantifying the duration and intensity of heat flux required for ignition of a material that is being evaluated. The equation was originally derived from radiant flux, but Cohen (2004) has shown it to be applicable for total flux (radiant

and convective). [10] This allows a comparison of both low-intensity prolonged exposures as well as high-intensity brief exposures against a constant to predict whether ignition will occur in a theoretical or test situation.

The constant that the measured value FTP is compared against is FTP_{ig} . This number represents the total value of $kW \cdot s/m^2$ at which ignition for a given material is predicted to occur. The FTP equation is as follows:

$$\int_{t_0}^{t_f} \delta(\dot{q}'' - \dot{q}_{cr}'')^{1.82} dt \geq FTP_{ig} \quad (8.1)$$

Where $\delta = 0$ for $\dot{q}'' < \dot{q}_{cr}''$

And $\delta = 1$ for $\dot{q}'' \geq \dot{q}_{cr}''$

For heat flux values below the critical flux, there will be no growth in the FTP and ignition will not be possible, regardless of how long the heat flux is applied. Starting at the point where the critical heat flux is reached, the integral is summed, less the critical flux value. This can be illustrated with an FTP curve which increases over time, with a slope related to the heat flux; higher heat fluxes will naturally have a steeper FTP curve slope, and as such will reach FTP_{ig} and ignition more rapidly. The point where the FTP curve crosses over the FTP_{ig} line, as shown in Figure 8.1, corresponds to the predicted time of piloted ignition. Note that the values do not represent actual test results or real-world FTP values; they are for illustrative purposes only.

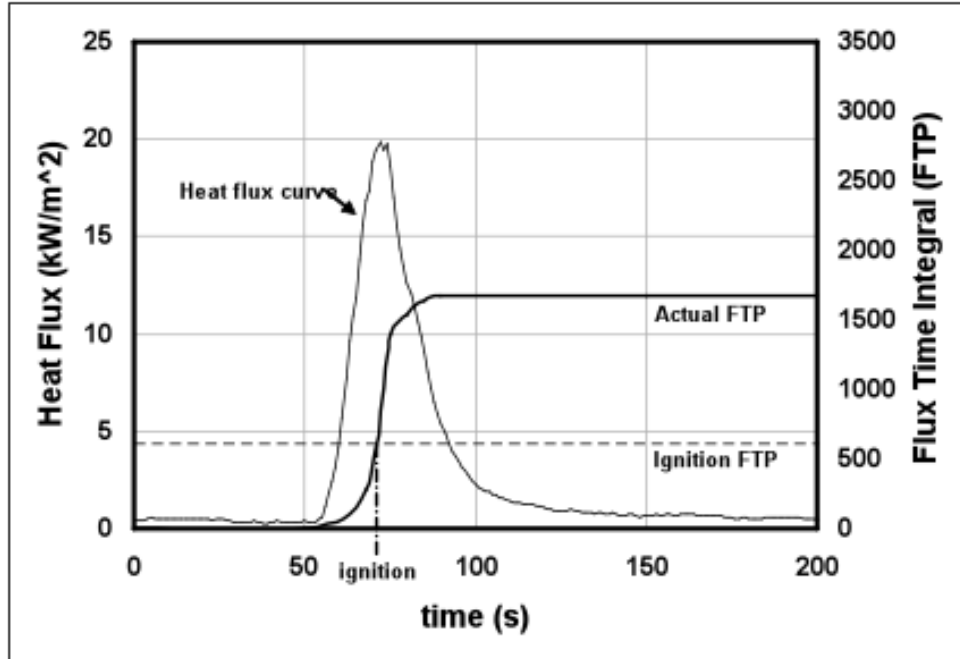


Figure 8.1: Flux-Time Integral (FTP) example showing the relationship between heat flux, FTP-ignition and predicted ignition time

Calculating the critical heat flux and FTP_{ig} for Douglas-fir was done by bench-scale testing. As documented in Modeling Ignition of Structures in Wildland/Urban Interface Fires (Tran 1992) [1], ignition tests were done that involved a fixed radiant flux and a vertical sample. The time to ignition (t_{ig}) was obtained as a function of heat flux. Based on the work of Janssens [15], [16] a correlation of $(1/t_{ig})^{0.547}$ versus heat flux was used, which led to the following relationship:

$$(t_{ig})^{-0.547} = a\dot{q}_e'' + b \quad (8.2)$$

Where for Douglas-fir plywood $a=0.006006$ and $b=-0.0789$. The intercept with the abscissa is equal to the critical heat flux, \dot{q}_{cr}'' , which in this case is 13.1 kW/m^2 . For ignition at a steady heat flux the following equation results:

$$(q_e'' - q_{cr}'')^{1.828} t \geq a^{-1.828} \quad (8.3)$$

Therefore, $FTP_{ig} = a^{-1.828}$. In the case of Douglas-fir wood $FTP_{ig} = 11501$. This is the value against which the area under the head flux curve will be compared to determine if ignition is possible.

The implications for the FTP as related to this body of work are limited, as we are dealing with single tree fires which are not likely to have an impact on a structure in the WUI by themselves – in fact the heat flux recorded does not go over the minimum critical heat flux value for plywood. However, empirically determining the FTP_{ig} value for shrubs or other trees, or even grasses may allow the threat of fire spread to be quantified. Based on the heat flux values recorded in this series of tests, and the typical time frame of 60 seconds, FTP values can be calculated to other FTP_{ig} to predict if ignition is likely.

Additionally, once multiple trees are involved, or the scale of the tree is greatly increased, calculating the FTP can be of aid to predict the distance needed between a structure and a body of trees to ensure that piloted ignition is not a high risk.

Bibliography

- [1] 1st International Fire and Materials Conference. *Modeling Ignition of Structures in Wildland/Urban Interface Fires*, Arlington VA, 1992. [2.1.3](#), [8.1](#)
- [2] 2nd Fire Ecology Congress. *A Review of Error Associated with Thermocouple Temperature Measurements in Fire Environments*, Boston, MA, 2003. American Meteorological Society. November 16–20. [6.1](#)
- [3] F. Albini. Spot fire distances from burning trees – a predictive model. Technical report, USDA Forest Service, 1979. [3.2.1](#)
- [4] V. Babrauskas. *The SFPE Handbook of Fire Protection Engineering - Heat Release Rates*. National Fire Protection Association, Quincy, MA, Third edition, 2002. [1](#), [2.1.1](#), [3.2.1](#)
- [5] V. Babrauskas, G. Chastagner, and E. Strauss. Flammability of cut christmas trees. Unpublished. [2.1.1](#), [3.2.1](#), [4.2.3](#)
- [6] S. Badger. Large-loss fires in the united states. <http://www.nfpa.org>, November 2004. [1](#)
- [7] D. Baily and R. Montague. *Fire Protection Handbook – Wildland Fire Management*. National Fire Protection Association, Quincy, MA, nineteenth edition, 2000. [1](#)
- [8] E. Baker. Phone conversation with G. Chastagner, 12 2004. [8](#)
- [9] M. Clark, T. Fletcher, and R. Linn. A sub-grid, mixture-fraction-based thermodynamic equilibrium model for gas phase combustion in FIRETEC: development and results. *International Journal of Wildland Fire*, 19:202–212, 2010. [2.2](#)
- [10] J. Cohen. Relating flame radiation to home ignition using modeling and experimental crown fire. *Canadian Journal of Forest Research*, 34:1616–1626, 2004. [2.1.3](#), [8.1](#)
- [11] G. Damant and S. Nurbakhsh. Christmas trees what happens when they ignite? *Fire and Materials*, 18:916, 1994. [1](#)

- [12] M. Etlinger. Fire performance of landscape plants. Master's thesis, University of California, 2000. MS Thesis in Wood Science and Technology. 1, 2.1.2
- [13] G. Heskestad. Dynamics of the fire plume. *Philosophical Transactions: Mathematical, Physical and Engineering Sciences*, 356:2815–2833, 1998. 5.1, 5.1
- [14] IAWF. *Modeling Potential Structure Ignitions from Flame Radiation Exposure with Implications for Wildland/Urban Interface Fire Management*. 13th Fire and Forest Metrology Conference, 1996. 2.1.3
- [15] International Conference on Fires in Buildings. *Use of Bench-Scale Piloted Ignition Data for Mathematical Fire Models*, Lancaster PA, 1989. Techomic. 8.1
- [16] M. Janssens. *Fundamental Thermophysical Characteristics of Wood and their Role in Enclosures Fire Growth*. PhD thesis, University of Gent, Belgium, 1991. 8.1
- [17] C. Jennings. Development of protocols for testing the exterior components and assemblies of residential structures under simulated wildfire conditions. Master's thesis, University of California, 2000. MS Thesis in Wood Science and Technology. 1
- [18] R. Linn. *A transport model for prediction of wildfire behavior*. PhD thesis, New Mexico State University, USA, 1997. 2.2
- [19] W. Mell, S. Manzello, A. Maranghides, D. Butry, and R. Rehm. The wildland-urban interface fire problem – current approaches and research needs. *International Journal of Wildland Fire*, 19:238–251, 2010. 2.2
- [20] P. Peper and G. McPherson. Evaluation of four methods for estimating leaf area of isolated trees. *Urban Forestry and Urban Greening*, 2:019–029, 2003. 3.2.4
- [21] W. Pitts, E. Braun, R. Peacock, H. Mitler, E. Johnsson, P. Reneke, and L. Blevins. *Thermal Measurements: The Foundation of Fire Standards – Temperature Uncertainties for Bare-Bead and Aspirated Thermocouple Measurements in Fire Environments*. ASTM STP 1427. ASTM International, West Conshohocken, PA, 2002. LA Gritzso and NJ Alvares, editors. 6.1
- [22] S. Pyne, P. Andrew, and R. Laven. *Introduction to Wildland Fire*. John Wiley and Sons, New York, second edition, 1996. 2.2, 3.2.1
- [23] SILVIS Lab. Wildland-urban interface maps, statistics, and data. <http://silvis.forest.wisc.edu/Library/WUILibrary.asp>, November 2004. 1

- [24] D. Stroup, L. DeLauter, J. Lee, and G. Roadarmel. Scotch Pine Christmas Tree Fire Tests. Report of Test. FR 4010, 1999. [1](#), [2.1.1](#), [3.2.8](#)
- [25] D. Stroup, L. DeLauter, J. Lee, and G. Roadarmel. Large fire research facility (building 205) exhaust hood head release rate measurement system. Technical report, NIST, National Institute of Standards and Technology, 2000. [6.3](#)
- [26] W. Walton, D. Carpenter, and C. Wood. *Fire Protection Handbook – Deterministic Computer Models*. National Fire Protection Association, Quincy, MA, nineteenth edition, 2000. [2.2](#)
- [27] D. Weise, R. White, F. Beall, and M. Etlinger. Seasonal changes in selected combustion characteristics of ornamental vegetation. Technical report, USFS (American Meteorology Society), 2003. [3.2.4](#)